National Academy of Sciences of Ukraine
The A.N. Podgorny Institute for Mechanical Engineering Problems

B.A. TROSHENKIN

RENEWABLE ENERGY

IN 2 PARTS

PART 1

THERMODYNAMICS OF THE OCEAN AND THE ATMOSPHERE. OCEAN THERMAL ENERGY CONVERSION PLANTS

Translated from the Russian
By
V.A. OBRISAN

Kharkov
Fort Publishers
2003

UDC 551.551+551.583+621.311.21(26)+621.483(26)
LBC 31.55
Ò76

Reviewers:
A.L. Shubenko, Doc. Sc. (Eng.), Prof., Head of Department for Optimization of Processes in and Design of Turbomachines at IPMash NAS of Ukraine;
V.P. Shaporev, Doc. Sc. (Eng.), Prof., Head of Chair for Chemical Engineering and Industrial Ecology at the National Technological University "KhPI".
Recommended for printing by the Scientific Council of the A.N. Podgorny Institute for Problems in Mechanical Engineering (Protocol No. 4 of 9 July 2003)

Troshenkin B.A.

T76 Renewable Energy. In 2 parts. — Part I — Thermodynamics of the Ocean and Atmosphere. Ocean Thermal Energy Conversion Plants. — National Academy of Sciences of Ukraine. A.N. Podgorny Institute for Mechanical Engineering Problems. — Kharkov: Fort Publishers, 2003. — 100 pp.
ISBN 966-02-3053-2
ISBN 966-02-3054-0 (Part I)
ISBN 966-7097-88-9

Since the moment of its emergence, the development of the Solar system, and in particular of the Earth, has been strictly governed by the laws of thermodynamics. These laws govern the behavior of ocean waters, the Earth's crust, and Nature. Based on *i*-thermodynamics, the monograph exposes the effect of ocean and atmospheric currents on Earth's rotational speed, gives an explanation for ancient floods and glaciation, and establishes the atmosphere's chemical composition during the period of formation of coal, oil and gas deposits. The sites of ocean thermal energy conversion plants, which would not affect Earth's climate, have been identified. The most effective methods of recovering natural energy have been substantiated. In turn, μ-thermodynamics has made it possible to assess the rate of formation of Earth's crust and associated therewith periods of volcano eruptions and earthquakes. As a rule, seismic zones correspond to geothermal heat sources. An analysis of the cycles of power plants utilizing Earth's heat has been presented.

The monograph is intended for experts in Earth-related power and physics problems as well as for those readers in geophysics who have a solid background in this area. It can also benefit students of higher education institutions.

UDC 551.551+551.583+621.311.21(26)+621.483(26)
LBC 31.55

ISBN 966-02-3053-2
ISBN 966-02-3054-0 (×. 1)
ISBN 966-7097-88-9

PREFACE

This book is based on lectures given by the author at the National Technological University "KhPI" in the course "Ecological Problems in Non-Conventional Power Engineering". The structure of the lectures assumes that the students have a definite level of knowledge in physics, and are keen on investing the surrounding world.

The author invites students, who have armed themselves with the laws of energy conversion as a guide, to go on a fascinating tour of the expanses of the ocean and the atmosphere, and of the Earth's depth. For in-depth knowledge, the program of the tour includes visits to Jupiter and Mars.

Acquiring knowledge of the theoretical basics of natural processes is backed up with information on the results of testing pilot models, and examples of design, the majority of which have been taken from the author's monograph published earlier (Circulation and Film Evaporators, and Hydrogen Reactors).

It is supposed that, in returning from the tour, the participants will be fairly well trained and able to identify the sites of renewable energy sources on their own.

Further, they will be familiarized with the most effective methods of recovering this energy without disturbing the environmental equilibrium.

When investigating the processes in the lithosphere, the students will get to know the regularities of location of geothermal heat sources, and how to utilise their energy. Students' attention is drawn also to the consequences of non-controlled exploitation of natural resources.

It is the author's hope that this textbook will benefit experts in different areas of Earth Science.

Acknowledgments

The author expresses his gratitude to the staff of the Laboratory for Alternative and Renewable Energy Sources of the A.N. Podgorny Institute for Mechanical Engineering Problems of the NAS of Ukraine for their advice, and for participating in a series of experiments. The author also appreciates the efforts of the reviewers and editors.

KEY SYMBOLS AND ABBREVIATIONS:

D is apparatus diameter, m
Dia. is tube diameter, m
L is length, m
H is height, m
δ is thickness, or length increment, m
P is perimeter, m
F is area, m^2
f is cross section area, or unit surface, m^2
τ is time, s
G is mass flow rate, kg/s
V is volumetric flow rate, m^3/s
M is mass, kg; or molar mass, kg/mol
m is reflux density, or fluid volumetric flow rate per unit length of the perimeter of the cross section of heat transfer tubes, $m^3/(m \cdot s)$ or $kg/(m \cdot s)$
υ is velocity, m/s
x is mass vapor content
β is vapor volumetric flow ratio
φ is gas volume fraction
E is absolute splash entrainment, m^3/s; or activation energy
μ_e is efflux coefficient
θ is wetting angle, deg
p is pressure, Pa
Δp is channel flow resistance, N/m^2
t is temperature, °C
Δt is temperature difference, °C
T is temperature, K
R is gas constant, J/(kg K); or radius, m
Gi is Gibbs energy, J
K is equilibrium constant
μ is chemical potential, or specific chemical affinity, J/kg; or dynamic viscosity, Pa • s
ν is kinematic viscosity, m^2/s; or stoichiometric factor
i is enthalpy, J/kg
h is enthalpy variation, J/kg
r is heat of vaporization, J/kg
S is entropy, J/(kg • °C)

η is efficiency

Q is heat flux, W

q is heat flux density, W/m^2

α is calorific efficiency, $W/(m^2 \cdot ^\circ C)$; or fraction of reacted substance, or substance decomposition depth

W is outgassing rate, $m^3/(kg \cdot s)$, $m^3/(m^2 \cdot s)$

κ is velocity constant, or coefficient/factor

ε is heat resistance, $m^2 \cdot ^\circ C/W$

λ is thermal conductivity, $W/(m \cdot ^\circ C)$

c is heat capacity, $J/(kg \cdot ^\circ C)$

ρ is density, kg/m^3

σ is surface tension, kg/m

g is gravitational acceleration, m/s^2

Subscripts and superscripts

L is liquid

G is gas

mx is mixture

i is conditions on the inner wall side

e is conditions on the outer wall side

p is wall

av is average value

cr is critical value

sp is specified value

fr is friction

max is maximum

min is minimum

o is outflow

red is reduced

D is diffusion

C is concentration

One stroke designates a liquid-related value

Two strokes designate a vapor-related value

INTRODUCTION

Since the moment of its emergence, the development of the Solar system, and, in particular, of the Earth, has been strictly governed by the laws of thermodynamics. These laws govern the behavior of the ocean waters, the atmosphere, the Earth's crust, and of animate nature.

Meanwhile, the majority of investigations lack analysis of the energy characteristics of Earth's processes being observed. This fact impedes the solution of a number of practical problems. The major challenge is providing industry with raw materials and energy. As well known, the development of civilization has led to a dramatic depletion of natural resources and to environmental contamination. Such consequences could have been avoided if renewable sources of energy and raw materials were developed.

The object of this study is to trace the paths of energy conversions on Earth, and to identify the conditions of utilizing renewable energy and raw materials.

In the first place, one's attention is drawn to the energy of ocean currents and airflows as well as to the temperature gradient between water layers in the ocean.

The World Ocean is known to cover 71 % of Earth's surface, receiving, hence, the major influx of solar radiation energy. Due to equilibrium between absorption of solar radiation, on the one hand, and the long wave radiation of the sea's surface and evaporation, on the other hand, a steady thermal state of the seas is maintained. This state is characterized by heating of the ocean surface water in tropical and subtropical regions to 25 to 30 °C, whereas at the depths of 400 to 500 m, the water temperature is 4 to 10 °C. This temperature difference can be harnessed for generating energy.

In this connection, we are facing the problem of assessing the admissible limits of utilizing this energy without disturbing Earth's ecological equilibrium.

It is necessary to determine the sites of ocean thermal energy conversion (OTEC) plants and of industrial facilities for manufacturing commercial products by utilizing OTEC plant-generated electric power.

Besides, it will be necessary to master the methods of controlling the ocean's surface layer temperature with floating OTEC plants to prevent the occurrence of storms and hurricanes.

The first part of the monograph deals with the solution of these problems.

Another, no less important source of renewable energy is Earth's heat. The overall heat radiation background is known to be created by radioactive

substances scattered in the Earth's crust. However, for such energy-intensive processes as earthquakes and movement of continents to occur, additional energy sources are required. The initiators of such impressive events are believed to be reactions occurring several hundred kilometers deep. The most likely of these reactions are those of oxidation of some basic Earth's elements.

During these reactions, part of the chemical energy is converted to mechanical energy spent on displacing Earth's strata, whereas the other part is liberated in the form of heat. Hence, knowing the rate of underground reactions makes it possible to predict the terms of earthquakes.

As a rule, high-seismicity zones are associated with geothermal zones that accumulate heat yielded by reactions.

Though the majority of deep heat sources have been well investigated, the environmental effects of their utilization by the hole drilling method are not yet sufficiently clear.

Roughly the same situation is developing during large-scale extraction of mineral deposits from the Earth.

Here an energy evaluation of changes occurring in nature is also needed.

The same analysis allows to assert that coal, oil and gas deposits are the milestones that point to Earth's transition, as a material system, from one energy state to another. These transitions also involve changes in the composition of the atmosphere, which, in turn, intensify, or mitigate, the greenhouse effect.

These issues are dealt with in the second part of the book.

Let us dwell on the methods of solving the problems stated.

The methods accepted are based on the notion that the laws of thermodynamics govern any natural process on Earth, ultimately.

Let us examine the process of natural circulation of flows. The phenomenon of natural circulation, in terms of energy, is reduced to the Carnot principle. It is natural circulation that leads to an increase in entropy of these processes, i.e. to their irreversibility. Considering the reversible thermodynamic cycle of this effect, one can establish the key regularities of flow movement in different media. Moreover, it turned out that acceleration of currents during water evaporation from the Ocean's surface, resulting in Earth's receiving a force impulse, depends entirely on a change in the medium's enthalpy.

For sake of simplicity, the section of investigations related to phase changes in the atmosphere and oceans is called i-thermodynamics (where i is the medium's enthalpy).

The section of physics known as "i-thermodynamics" gives an objective explanation of the regularities of circulation of water currents and airflows, ex-

tends our knowledge of secular climatic variations, and presents some ideas on the initial stages of Earth's development. A distinctive feature of processes related to *i*-thermodynamics is that the chemical composition of substances participating therein does not change.

The theory of thermodynamics acquires logical completeness when its provisions are extended to systems with a variable chemical composition. Thus, when substances interact underground, a physico-mechanical process of natural circulation of flows, on the one hand, and physico-chemical phenomena linked to restructuring of the electronic shells of the reacting components, on the other hand, are observed.

The thermodynamic method allows to determine the following: the energy capacity and the direction of chemical conversions, and the reaction-induced thermal changes; the stability of compounds formed; the maximum equilibrium concentrations of reaction products, and their ultimate yield; and the process optimal regime (temperature, pressure and concentration of reagents). The reactions are caused by the thermodynamic instability of a system made up of different substances. The measure of this instability is the free energy released during the reaction. In a reversible isothermal process, this energy is equal in absolute value, and inverse in sign, to the maximum effective work. The latter includes all the work performed during the process, apart from the expansion one.

As distinct from the case of phase conversions, to describe the behavior of systems with a variable chemical composition, μ-thermodynamics (where μ is the chemical potential introduced by J. Gibbs for evaluating the equilibrium of heterogeneous substances [1]) turned out to be more acceptable.

The method of μ-thermodynamics of reversible processes introduces some clarity to evaluating the power of underground heat sources, and allows to determine energy losses during earthquakes and volcano eruptions.

In both phase and chemical conversions, the methods used do not contain the physical parameter of time. Time, as a parameter of the system's state, is indicative of actual flow from the past to the future in irreversible and continuously running processes of interaction of systems having different temperatures, pressures, concentrations, or chemical potentials. The direction of flow of time, which coincides with entropy growth for each environmentally isolated system, is known as the future by the definition given in [2]. Until physical and chemical gradients exist, a time gradient will also be present. With disappearance of these gradients, time, as a physical parameter of evolution of a contacting system, disappears as well.

Gradients, as motive forces, are maintained in the environment by two energy sources, viz. the Sun and exothermal reactions in the Earth's deep. The ideal reversible cycle of heat transfer from the equator to the poles consists of several stages, each of which correspond to its energy losses that convert the cycle ultimately to an irreversible one. Due to friction, the kinetic energy of flows, moving with definite velocity, are converted again to heat absorbed by the environment.

The resistance of water and air masses to the movement of flows is evaluated by empirical formulas found experimentally. The time of completion of a non-ideal cycle consists, accordingly, of the time of running of separate processes.

From the above, it follows that an estimate of the time of occurrence of an event in the atmosphere, or in the ocean, at the current stage of development of physics, has a semi-empirical character.

Roughly, the same situation exists in methods for evaluating variable-component systems inherent to the lithosphere. Moreover, for these systems there is no clearly defined relation between the flow velocity, and the rate of substance interaction. Discontinuity (discreteness) of matter makes it possible for the particles of the components of each system to be spatially arranged to definite laws, and to react over a specific time interval. This interval defines the formal relationships that describe the process.

Using formal kinetics relationships is, in itself, a manifestation of the poor development of methods in thermodynamics of irreversible processes. In other terms, the principle of least dissipation of energy, originating apparently from the principle of least action in mechanics, is insufficient alone for compiling strict analytical relationships. Moreover, the principle considered is true only for systems with insignificant deviation of parameters from equilibrium conditions.

Meanwhile, extensive experimental data point to the close relation between the rate of phase and chemical conversions, and the magnitude of the available chemical potential. In μ-thermodynamics analysis, this made it possible to establish several relationships for systems comparatively far from the state of equilibrium. Hence, this allowed to refine specific provisions in the thermodynamics of irreversible processes when considering processes in the lithosphere.

The movement of water and air currents cannot be explained rationally without knowing the laws of their distribution and circulation in the atmosphere and ocean. The word "distribution" means an ordering of flows in space, and the word "circulation" means the regularity of passage of separate flow ele-

ments over fixed Earth zones. In essence, investigating the ocean's state is reduced to searching for a spatial symmetry of water structures, and for the periodicity of effects in these structures. The predominant symmetries in the arrangement of flows are the bilateral (mirror), rotational and translatory ones. The general laws of mechanics define the theoretical model of circulation of water masses in an ocean with an even bed, which, by assumption, spreads over the entire Earth's surface. Actually though, the continents and islands introduce substantial deviations to the ideal flow distribution pattern. To estimate the degree of deviation from the laws of symmetry, the distribution and circulation of currents on Jupiter were analyzed.

Momentum exchange between the warm currents and the Earth, and transfer of this momentum to cold currents is linked, in any event, to Earth's axial rotational speed.

Of definite interest is studying the regularities of current circulation at the early stages of Earth's development. Rotating fluid bodies are known to become flattened at the poles. For example, there is a difference between the polar and equatorial diameters of the Earth. This difference appeared as far back as when the Earth was in a molten state.

It seems that the circulation of currents on the molten Earth differed but little from that at present. Therefore, the presentation of material referring to the formation of continents during Earth's cooling period is also based on *i*-thermodynamics. In so doing, the elements of "symmetry" and "asymmetry" were accounted for in the structure of the currents.

Yet the Earth is a fairly massive celestial body, for whose spin-up (in the absence of mountains) the amount of mechanical energy released during redistribution of low-potential heat is insufficient. The latter condition leads to events of long ago, viz. to the time of Earth's creation. In this connection, an approximate estimate of Earth's initial angular momentum was made. The estimate is based on the theory advanced by V. Ambartsumian, and on S. Hawking's suggestions, as those, which best reflect the basic principles of thermodynamics [3 and 4].

Application of geometrical principles is also appropriate for examining processes in the lithosphere. In this case, the arrangement and height of mountain ranges carry information on the force and direction of natural circulation of flows in the Earth's deep. However, in so doing, the investigation methods tend to rely on chemical potentials as the motive forces of the processes.

Studying the regularities of crystallizing of substances in cooling flows makes it possible to evaluate the distribution of Earth's mineral resources.

To achieve completeness of the results obtained, a comparison was made of the basic characteristics of the process of volcano eruptions on Earth, and those on Mars that occurred earlier.

In some cases, the measure of irregularity of flows is linked to the notion of configuration entropy introduced to the kinetic theory of gases. Hence, reduction in flow distribution irregularity involves a decrease in entropy.

Physical laws are known to be observed in both natural and man-induced conditions. Therefore, among engineered devices, one can always find objects, wherein the process runs identically to some natural process. Especially suitable for comparison are evaporation installations, wherein circulation of flows occurs at extremely small temperature differences.

The comparison method is straightforward and robust. Moreover, some processes that occur spontaneously in the atmosphere and oceans can be explained only by a priori thermodynamic analysis with subsequent verification of findings on laboratory, pilot and commercial test stands. Experimental methods of investigating processes occurring in the lithosphere are somewhat different from the previous ones. The experimental equipment required here includes electric heating furnaces and high-pressure chemical reactors. To simulate natural processes, several alloys and their respective oxide systems were developed a priori.

The monograph also discusses the problem of oil and gas formation. With this in view, biological systems, in particular, hydrogen-oxidizing bacteria were used. Testing the biological reactor allowed to establish the kinetic characteristics of the process of conversion of inorganic components and carbon dioxide to organic matter. Besides, some notions on the thermodynamics of live systems were refined.

For fairness' sake, it should be noted that the methods of analyzing natural processes developed here are approximate ones, since thermodynamics points only to the most probable course of events, without ruling out other ones.

CHAPTER 1

NATURAL CIRCULATION OF FLOWS

Let us consider the process of natural circulation of flows both in natural and man-induced conditions.

1.1. CIRCULATION OF FLOWS IN A GEOTHERMAL LAKE

Assume that in the mountains there is a lake supplied with warm water (Fig. 1). Let us investigate the stability of water layers with respect to forces inducing natural circulation of flows. The practical value of this investigation is in obtaining baseline data for designing a geothermal electric power plant and, in particular, wells for extracting hot water.

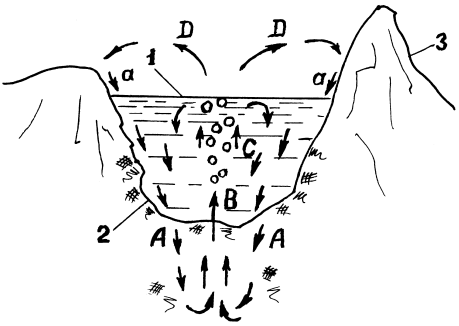

1 – lake; 2 – lake bottom; 3 – mountains; A – cold water inflow to the Earth; B – hot water outflow from the Earth; C – vapor-liquid flow in the lake's centre; D – vapor flow rising to the atmosphere; a – rain water flowing into the lake.

Fig. 1. Scheme of flows in a natural lake

The mathematical description of hydrodynamic instability in a mountain lake can be considered as a simplified model of processes in the lithosphere. However, the principal objective of investigating circulation is developing an analog, by comparison with which it will be easier to establish the regularities of flow motion in the atmosphere and the World Ocean.

Under normal conditions, fine natural circulation is present in a mountain lake. But if superheated water were to flow into the lake (arrow B), it would boil. A high-speed rise flow appears (arrow C), which sharply intensifies water circulation. The boil vapors rise to the atmosphere, condense there, and in the form of rain or mountain streams, return to the lake (arrow a). The cooled circulating water flow (arrow A) descends again to the bottom of the lake. Visually, this event suggests the simple idea that appearance of vapor bubbles in liquid reduces the medium density in the rise channel. (The channel boundaries are the immobile liquid layers.) As a result, the weight of the vapor-liquid mixture column in the rise channel turns out to be less than that of the pure water column in the descend channel, which, apparently, is the motive force of natural circulation.

Nevertheless, such an evident circulation pattern is not altogether correct. The process pattern presented relates to incompressible fluids. With appearance of vapor in the system, the explanation of the regularities observed goes from the area of hydrodynamics to the area of gas dynamics. Let us demonstrate the drawbacks of the hydrodynamic model by example of natural flow circulation design in an evaporator installation.

1.2. EVAPORATOR WITH NATURAL FLOW CIRCULATION

To start with, the notion "density of a medium in the rise channel" has no physical sense. This density cannot be measured, since there are two media in the rise channel, viz. vapor and liquid. The liquid density in the circuit changes but slightly, hence formation of bubbles in the rise channel has no significant effect on the hydrostatic pressure in the liquid column. In turn, the vapor density turns out to be higher in the boil zone than over the lake's surface.

A more precise physical model can be formulated as follows: the motion of a medium in a circuit with natural flow is caused by vapor expansion at a pressure differential acting in the beginning and in the end of the boil channel. This differential is caused by conversion of part of the thermal energy transmitted from the Earth's deep to the atmosphere, to mechanical energy of compressed vapor. The differential head thus created under stationary conditions is equal to the sum of hydraulic resistances in all circuit sections and working medium acceleration losses.

When designing evaporators using the systematic approach, first it is necessary to determine the amount of energy available. Fig. 2 shows the diagram of an evaporator installation.

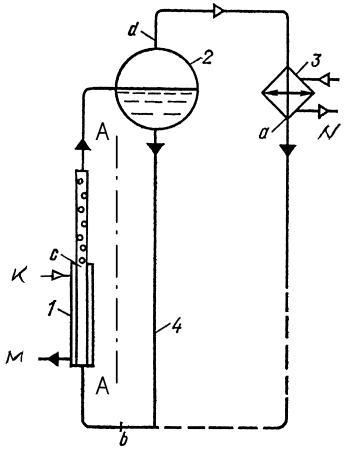

1 – heated channel; 2 – separator; 3 – condenser; 4 – downtake channel; c – solution boil zone; d – vapor outlet to the condenser; a – condensate outlet to the downtake pipe; b – lower bend of the flow circuit; K – vapor; M – condensate; N – water; AA – flow circuit plane of symmetry.

Fig. 2. Diagram of an evaporator's flow circuit

A visual presentation of the scale of commercial installations employed is given in Fig. 3. The picture shows six-vessel evaporator installations for producing fresh water. The daily capacity of each installation is 120,000 m^3.

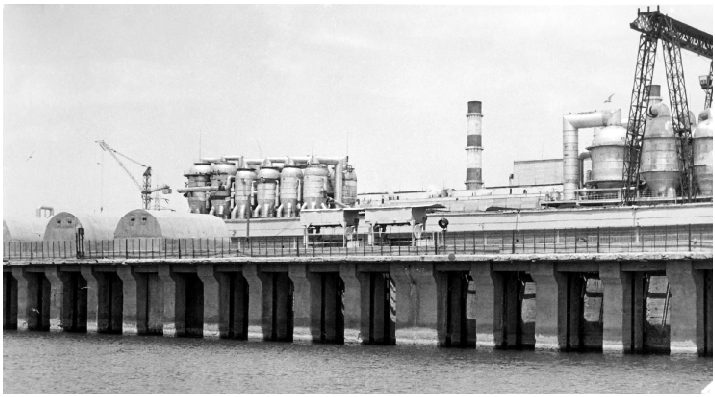

Fig. 3. General view of six-vessel evaporator installations for producing fresh water (photo by Novikov Ye.P., Shevchenko City)

1.2.1. Analysis of the evaporation cycle

The installation cycle in T–S coordinates, when the boil zone is beyond the heating chamber, is shown in Fig. 4. The cycle combines four processes: a–b is adiabatic pressure increase in the downtake channel under gravitational

effect (at an extremely small liquid temperature increase); b–c is solution heating in the chamber at a small pressure difference; c–d is adiabatic expansion of evaporator vapor in the rise channel (isoentropic process); cz is vapor expansion with friction energy loss (polytropic process); cn is flow throttling in the rise channel (isoenthalpic process); da is evaporator vapor condensing in condenser 3 (isobaric-isothermal process).

The temperature increase during flow compression is so small that, practically, points a and b merge to one point. Therefore, the cycle can be called a triangular one. Curve x = 0 (lower boundary curve) separates the water zone from the saturated vapor zone.

Heat q_1, transferred to the solution during process a–b and b–c, is shown by area abcdfka, and it is found from formula $q_1 = i_c - i_a$. Heat q_2, released by evaporator vapor to the condenser (area adfka), is found from relationship $q_2 = i_d - i_a$. Under these conditions, heat converted to work in the ideal cycle (area abcda), is $q_1 - q_2 = (i_c - i_a) - (i_d - i_a) = i_c - i_d = h$.

The heat efficiency of the installation's actual cycle is found from the formula

$$\eta_t = \frac{q_1 - q_2}{q_1} = \frac{i_c - i_d}{i_c - i_a} = \frac{h}{i_c - i_a}.$$

When considering the evaporator installation cycle, it was accepted that in the rise channel there takes place adiabatic vapor expansion without internal losses (reversible). In fact, this process is an irreversible one due to internal losses. The conventional graph of an irreversible process is shown in Fig. 4 by sloping line cz. The full cycle in the diagram, at irreversible expansion, occupies the area abczda. The efficiency of this cycle is found from the formula

$$\eta_{tz} = \frac{q_1' - q_2'}{q_1'}.$$

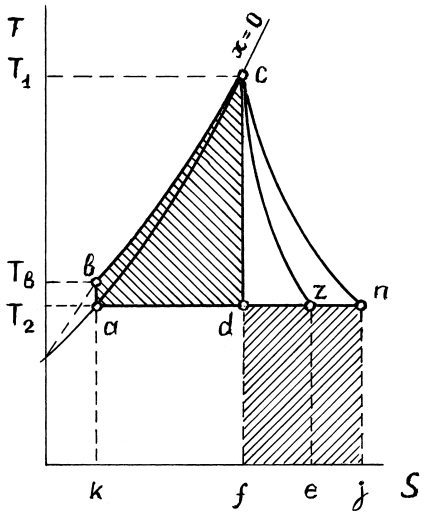

Fig. 4. Evaporator installation cycle with natural flow circulation in the T–S coordinate system

Heat q'$_2$, transferred during process za to the condenser, is shown by area zekaz. Since area adfka is smaller than area zekaz, $\eta_{tz} < \eta_t$. The efficiency of an actual cycle is

$$\eta_{tz} = \frac{i_c - i_z}{i_c - i_a} = \frac{h_z}{i_c - i_a}.$$

The ratio of the thermal efficiency η_{tz} of the cycle at irreversible vapor expansion to the thermal efficiency η_t of the cycle at reversible expansion is known as the internal thermal efficiency:

$$\eta_{i.e} = \frac{\eta_{tz}}{\eta_t} \text{ or } \eta_{tz} = \eta_{i.e} \cdot \eta_t.$$

In the rise channel, liquid flows from the initial level in the boil zone to the level in the separator by overcoming the force of gravity. In addition, the 2-phase flow is accelerated, and hence, effective work is performed.

It is only in the cn isoenthalpic throttling process that the flow is not accelerated. In this case, area njfdn, representing the amount of heat generated by friction, is numerically equal to area cdabc, corresponding to the amount of heat, which could have been converted to work in the adiabatic process cd.

During throttling, the flow entropy achieves its maximum value.

As a first approximation, it can be accepted that the internal efficiency $\eta_{i.e}$ of the rise channel is equal to the air-gas lift efficiency. For air-gas lifts with channels close in dimensions to those of evaporator channels, this efficiency varies within $\eta_{i.e} = 0.1$ to 0.3 [5]. The design valuesh, η_t and $\eta_{i.e}$ make it possible to proceed with gas-dynamic calculations. For this, the cycle diagram in the p—V coordinate system is used (Fig. 5).

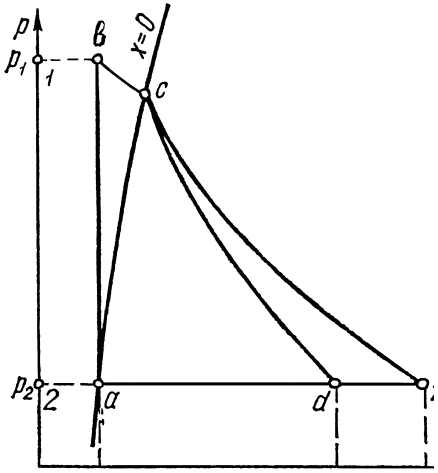

Fig. 5. Cycle of evaporator installation with natural circulation in the p —V coordinate system

For the reversible cycle, the work expended in the circuit on flow circulation, is equal to area abcda, deter-

mined as the difference of area 1bcda21 and area 2ab12, representing the work of the gravitational field in the downtake channel. The adiabatic compression process in diagram p–V is shown by isochore ab.

A decrease in compression work, at complete condensing, is due to the liquid being practically incompressible, and hence, all the work expended during compression is reduced to its pushing work. But since the liquid specific volume is small, the pushing work, equal to $(p_1 - p_2)V_a$, will also be small.

In the heating chamber, the water temperature rises, making its volume to increase (process bc). The change in density yields the so-called Archimedes's force, ensuring a weak flow circulation even prior to water boiling. For this flow regime, area abca should be approximately equal to area a21ba.

Intensive flow circulation is established under water boiling conditions. For a polytropic process, area abcza differs from area a21ba by the energy loss in the circuit corresponding to area czdc.

The effective work of vapor in the boil channel $h_z = \eta_{i.e}\, h$, where h is the work of evaporator vapor during reversible expansion. The values of h can be also calculated from the dependency $h = \frac{\upsilon_d^2 - \upsilon_c^2}{2}$, where υ_d is the outflow velocity of the liquid-vapor mixture at adiabatic reversible expansion; υ_c is the liquid velocity upstream the boil zone. Whence $\upsilon_d = \sqrt{2h + \upsilon_c^2}$; in an actual cycle $\upsilon_z = \sqrt{2\eta_{i.e}\, h + \upsilon_c^2}$.

Further, having the found flow velocity of the liquid-vapor mixture, for a concrete apparatus it is necessary to refine the channels' sections, assess the flow structure, and determine the hydraulic resistance of the circuit elements. Having refined the liquid superheating value, it is necessary to calculate once more the amount of energy available, and compare it with the spent one.

The effective work performed by evaporator vapor in the rise channel should ultimately be equal to the gravitational field work in the downtake channel. When evaporating a solution with a certain heat capacity, which defines the position of curve x = 0 on the T–S diagrams, the thermal efficiency increases with an increase in initial pressure p_c and a decrease in final pressure p_z. High pressures p_c correspond to higher circuits. In this case, the solution overheating temperature T_1 can be increased to increase the available heat difference.

At a constant heat load, circuit height reduction displaces the boil zone to the heating chamber. In so doing, the area limited by the cycle is reduced, and the thermal efficiency takes lesser values.

The same result can be achieved by increasing the amount of heat transferred from the heating chamber to the condenser at an invariable circuit height.

Testing a three-chamber model of an evaporator with a rise film can give an insight into the possibility of variating the values of the internal and thermal efficiencies. The apparatus consisted of three vertical tubes with the diameters $25 \cdot 10^{-3}$; $38 \cdot 10^{-3}$; and $57 \cdot 10^{-3}$ m, enclosed in separate heating chambers. The accepted length was 7 m, and the length of tubes dia. $57 \cdot 10^{-3}$ m was 7 and 9 m. In the upper part, the tubes being investigated were connected to one separator, and in the lower part, they were connected to one solution chamber.

Such design of the apparatus allowed conducting both joint and separate testing of tubes. Tests have shown that, at a pressure exceeding the atmospheric one, the lesser diameter tubes demonstrated a better performance. However, at vacuum increase and temperature difference decrease to 10 °C, the heat transfer in tube dia. $25 \cdot 10^{-3}$ m was significantly lower than in tubes with diameters $57 \cdot 10^{-3}$ m and $38 \cdot 10^{-3}$ m. Hence, reducing the water vapor elasticity makes the flow circuit internal efficiency drop. The condition can be corrected by replacing the gas-lift working medium — water vapor — with vapor of low-boiling liquids. Thus, if benzene, isoprene, chloroform, or any other liquid immiscible with the mixture, is introduced into the lower part of the heating chamber, the circulation rate increases dramatically [6]. This effect is accounted for by the higher vapor elasticity of the liquids mentioned as compared to that of water vapor at the same temperature conditions.

In turn, the thermal efficiency can be increased not only by increasing the flow circuit height, but also by changing the gravitational field intensity. Thus, circulation, for instance, of liquid hydrogen on massive planets will occur at higher rates than that on Earth.

The key regularities of the circulation process can be made more evident by considering an example of flow circuit design.

1.2.2. First-approximation circuit design

Initial conditions are specified for a concrete apparatus. Let us assume that an apparatus with a remote boil zone has been taken, and that the rise channel height is 2 m. The temperature of evaporator vapor in the separator is $t_2 = 100$ °C, and the solution flow velocity in the inlet section of the heat transfer tubes is $\upsilon_c = 0.5$ м/с. The product properties are taken into account.

First, these data are used to determine the hydrostatic pressure over the apparatus' height, and then to find the hydrodynamic pressure. With account of the solution's temperature depression and the hydrodynamic pressure, the

liquid temperature in the boil zone is found. We assume that at the boil point the product has the temperature of $t_l = 105$ °C, this approximately corresponding to the hydrostatic pressure of a 2 m water column.

The entropy of the vapor-solution mixture S_d, after adiabatic expansion, is equal to the entropy of the superheated liquid S_c in the boil zone: $S_d = S'_c = 1{,}363$ kJ/(kg °C).

The amount of evaporator vapor formed is found from dependence [7]

$$x = \frac{S_d - S'_d}{S''_d - S'_d} = 0.00928 \text{ kg}.$$

After expansion, the enthalpy of the vapor-solution mixture is

$$i_d = i'_d + r_d x,$$

where $r_d x$ is heat spent on evaporation; $i_d = 419.06 + 2{,}257.2 \times 0.00928 = 440.007$ kJ/kg. The heat difference $h = i'_c - i_d = 440.17 - 440.007 = 0.163$ kJ/kg. At adiabatic reversible expansion, the cycle thermal efficiency is

$$\eta_t = \frac{h}{i'_c - i'_a} = \frac{0.163}{440.17 - 419.06} = 0.0077.$$

At the internal thermal efficiency $\eta_{i.e} = 0.25$ [5], the actual thermal efficiency $\eta_{tz} = \eta_{i.e}\eta_t = 0.193$ %. At reversible expansion, the evaporator vapor work $h = 163$ J/kg. The evaporator vapor effective work in the riser channel $h_z = \eta_{i.e}h = 40.75$ J/kg.

The velocity of the vapor-solution mixture efflux to the separator, at adiabatic reversible expansion, is $\upsilon_d = \sqrt{2h + \upsilon_c^2} = 18.06$ m/s; in the actual cycle $\upsilon_z = \sqrt{2\eta_{i.e}h + \upsilon_c^2} = 9.02$ m/s.

Further, the velocity found is used to refine the flow structure and estimate the rise channel resistance. Liquid superheating and effective work are recalculated. Let us assume that the work value is the same as the previous one, i.e. $h_z = 40.75$ J/kg. The gravitational field work will be equal to hz if the hydraulic resistance of the downtake channel and of the riser channel upstream the boil zone will be 4 m of water column.

The design results obtained are compared with the data of the hydrodynamic model. The physical model of flow circulation in steam generators accepted in basic design can be formulated as follows: "Motion of a working medium in a circuit with natural circulation under the effect of gravitational forces arising due to a difference of medium densities in downtake — non-heated (or weakly heated) tubes, and rise — heated tubes; in stationary conditions, the

motive difference created thereby is equal to the sum of hydraulic resistances of all circuit sections and the working medium acceleration losses." [8]. Hence, hydrodynamic design is reduced to compiling and validating the balance of the specific energy of a non-stationary flow compressed in the channel riser section.

By standard analysis, it is possible to find the velocity of liquid efflux to the separator under the effect of the difference of medium column pressures in the rise and downtake channels. Assuming the rise channel to be filled with vapor from the point of liquid boil to the point of flow efflux to the separator, the difference of columns will be $\Delta p = 2$ m. Then the velocity of flow efflux to the separator $\upsilon = \sqrt{2g\Delta p} = 6.26$ m/s. With account of the rise channel efficiency $\upsilon = \sqrt{2g\eta_{i.e} \cdot \Delta p} = = 3.13$ m/s.

The efflux velocity, as per the standard method, cannot be higher than that found, since, according to hydrodynamics, there is no available energy to ensure flow motion. This calculation uses the difference of medium levels, whereas the previous one uses the vapor enthalpy difference. Wherefrom, standard analysis yields lower efflux velocities than that envisaged by thermodynamics, this accounting for differences in flow structures. It is this difference that yields errors in standard methods of steam generator and evaporator design.

The standard method's name "hydraulic design of apparatus" is incorrect since the laws of fluid mechanics (hydraulics) are in effect in the riser and downtake channels only to the boil zone, whereas further flow motion is governed primarily by gas dynamics laws.

Introducing the internal efficiency into design allows identifying the overall thermodynamic pattern of natural circulation without involved calculations of flow energy friction losses inside the channel. At the same time, the internal efficiency values have been established for a limited range of tube sizes, and have an approximate character. Due to this, more accurate methods of evaluating the flow resistances of channels have to be considered.

1.2.3. Second-approximation circuit design

Second-approximation design consists in refining flow resistance energy losses in a flow circuit.

The liquid flow resistance of the circuit's hydraulic part is evaluated by experimental data summarized, for example, in handbook [9].

Friction energy losses during two-phase flows in the vapor-liquid part of the circuit are calculated according to the data in [10 and 11].

In so doing, we take into account the gas volumetric fraction φ and the gas volumetric flow rate β. Calculation yields the excess resistance of channels to two-phase flows as compared to resistance to one-phase flows.

Tangential flow delivery to separator 2 gives rise to a rotating liquid swirl in its bottom part. The bulk of kinetic energy of a two-phase flow is converted, due to friction in the swirl, to heat, the remaining part being converted to potential energy of the downtake flow. Extensive studies have been conducted in estimating the resistance of the downtake channel inlet section to swirl displacement. Some of them will be used in the section on formation of continents.

Gas dynamic calculation yields the actual flow velocity in the flow circuit, after which the area of the evaporator heat exchange surface is found.

Similar calculation is required for determining the capacity of wells delivering heat to a geothermal power plant.

1.2.4. The features of a flow circuit as a thermal machine

Let us highlight some features of a flow circuit as a device for converting heat to work. Firstly, as distinct from thermal engines, the circuit cannot work without a gravitational field. At adiabatic expansion in the riser channel, the evaporator vapor, in lifting the liquid, overcomes the effect of the gravitational field, thereby yielding reserve work. After condensation (or vapor extraction), this reserve is used for liquid downtake. Since the mass of rise and downtake liquid is equal, the total work in the gravitational field circuit equals zero. However, the cycle thermal efficiency turns out to be dependent on the circuit height, and the liquid and vapor properties. The relative efficiency also depends on the geothermal features of the circuit, the properties of the vapor and liquid, and on their ratio over the rise channel height. Circulation occurs spontaneously due to tending of the system, which is in a gravitational field, to restore the disturbed equilibrium.

Secondly, at equal liquid levels in the rise and downtake channels, the U-shaped circuit ensures minimal energy expenditure on flow circulation. This shape is known to have bilateral (mirror) symmetry. In Fig. 2, AA is the mirror symmetry plane.

Thirdly, the circuit, as a rule, does not produce work that is external with respect to the installation, i.e. it is a closed system. Mechanical energy, produced by the heat of the heating vapor, is spent inside the circuit for flow circulation, and then it is converted again to heat received by the evaporator vapor. Of the available temperature difference, flow circulation claims its but insignificant part, whereas the main part is spent on heat transfer from the lake bottom to the water surface, and from water vapor to the mountains. As a result, the

work yield is clearly insufficient to return the system to its previous thermal state. Whence it follows that friction in the circuit channels, on the one hand, and temperature difference loss on the phase interface boundaries, on the other hand, convert the process of natural circulation of flows to an irreversible one.

In light of the ideas acquired, let us consider the circulation of flows on the nearest planets, for example, on Jupiter.

1.3. NATURAL CIRCULATION OF FLOWS ON JUPITER

Jupiter is the largest of the giant planets. Its mass is 318 times that of Earth. The gravitational acceleration on Jupiter exceeds that on Earth by a factor of 2.6. Jupiter's surface is covered by an ocean of liquid hydrogen.

The amount of heat received from the Sun per unit area is 27 time less than that received by a unit area on Earth. Such an amount of heat is capable of heating the ocean to the equilibrium temperature of 110 K. Meanwhile, direct measurements by both earth-based means and space probes indicate the temperature of 129 K. Higher temperatures have been detected near to the equator. Such a temperature can be accounted for only by a heat flow from the planet's deep, which exceeds the solar flow by a factor of two [12 and 13].

At the temperature of 129 K, atmospheric hydrogen is in a gaseous state. But, in descending into the planet's deep, hydrogen first passes into a liquid state, and then into a metallic one.

Since the bulk of heat is received from the core, liquid hydrogen should boil near to the boundary with the atmosphere. This makes it possible to use the technique developed for a geothermal lake to evaluate the natural circulation of flows on Jupiter.

All other conditions being equal, it can be stated that natural circulation in a vessel with liquid hydrogen on Earth will be less intensive than in natural conditions on Jupiter. In the latter case, the thermal efficiency of a circuit will be significantly higher.

Approximate data on the properties of liquid and gaseous hydrogen at the temperature on the phase interface boundary, which are necessary for calculation, can be obtained by extrapolating the values given in handbooks [14 to 17].

CONCLUSIONS

Let us sum up the investigation results. Thus, the state of water in a geothermal lake is unstable with respect to forces arising in the system when heat from underground flows to the bottom layers. Water circulation occurs spontaneously because the system, being in a gravitational field, tends to restore the disturbed equilibrium.

The efficiency of flow circuits with the boil channel height of $H = 2$ to 3 m is within $\eta = 0.1$ to 0.2 %. The efficiency grows with an increase of circuit height, pressure in the system, and gravitational field intensity.

Since gravitational instability occurs suddenly, when the system achieves a certain combination of parameters, the effect considered should be related to the category of spontaneous ones.

Let us agree calling further one or another natural phenomenon according to the kinds of forces that ensure flow delivery to the heating zone. In this case, cold water flows to the lake bottom under the effect of gravitational forces. Therefore, natural circulation of flows will be called the gravitational effect.

CHAPTER 2

THERMODYNAMICS OF THE OCEAN

The substance of this section of studies consists in proving the thesis that a planet with an atmosphere and an ocean, which is located close to a star, is unstable with respect to forces causing the planet to rotate about its axis.

So far, all the ideas on this problem fitted into the axiom: "Axial rotation is the common property of free bodies, one of the forms of their motion. Rotation occurs due to the velocity of particles, making up the body, necessarily having a component perpendicular to the radius. The composition of these components, according to the law of composition of vectors, defines the direction and angular velocity of a body's rotation." [18].

This statement relates only to the initial moment of planet formation, and helps little in clarifying its present state.

We shall have to ascertain that, under specific conditions, a planet receiving solar radiation should rotate spontaneously. At this, the angular velocity depends on the intensity of solar radiation, the planet's size and mass as well as on the properties of its gas-liquid shell.

2.1. REGULARITIES OF CURRENT CIRCULATION IN AN OCEAN

Natural phenomena on Earth are considered to have an intrinsic character. This is meant to be the most prevalent and faultless process of natural circulation of currents whose essence was considered in the preceding section.

The atmospheric processes being observed, however, are rather chaotic and depart significantly from laws of natural circulation.

The dynamics of the World Ocean waters fit the existing concepts to a still lesser extent. Earth's heating by the Sun makes the warm waters arrange above the cold ones, which, in itself, precludes the possibility of emergence of natural circulation. Meanwhile, intense currents cross the ocean in different directions, and on their boundaries with immobile layers, water swirls continuously emerge and disappear. Swirl formation is also wind-induced (Langmuir

circulation cells). The most intense sea current exists near the Antarctic shores (the circumpolar current) [19 to 21].

Clearly, energy is required for generating swirls and maintaining a certain current flow velocity. The dynamic processes in the ocean are reasonably assumed to be caused and maintained both by the energy of airflows and by partial utilization of the energy of Earth's rotation. The implication of such an approach is also evident, viz. continuous consumption of Earth's energy for formation and maintaining of water structures should invariably lead to a decrease in its rotational speed. Since this is not the case, there should be a mechanism of continuous replenishment of Earth's rotational energy with the Sun's energy, differing, however, from the mechanism of natural current circulation. We will assume a stagewise approach to solving this partial problem of elucidating the circulation mechanism.

2.1.1. The hydrodynamic circulation model

First, let us take, as a basis, the approximate hydrodynamic circulation model involving non-compressible liquids, and demonstrate its positive and negative aspects.

Assume we have a vessel with a vertical watertight partition; and that warm water is poured into one compartment, and cold water to the other one. Let us carefully pull out the partition. When mixing starts, warm water will attempt to occupy the upper level in the cold-water compartment, and cold water will flow over the whole bottom of the vessel.

As oceanologists assert, it is this phenomenon that causes warm water to move poleward, and cold water to move to the equator [22].

In the first approximation, let us be oriented to this, so-called "thermohaline" circulation.

In looking on Earth from above, one can see shallow seas located at the eastern shores of continents. These seas act as heat accumulators. The most intensive warm currents originate here. Moving in the northeastern and southeastern directions, these currents as if drag the Earth therewith, this determining its direction of rotation. Having received an impulse from the warm currents, Earth transfers it to the cold ones. In principle, this situation is shown in the p–V diagram (Fig. 5) by equality of areas bcab and a21ba (without account of friction in streams). Yet the forces moving the cold streams to the near-equator heating zone are now Earth's centrifugal forces.

It is to be borne in mind that, under natural conditions, water layers are located on a spherical rotating surface. Both kinds of currents participate in joint rotation with the Earth. Thus, the warm current at the equator has the linear

velocity of 464 m/s. In moving poleward, its distance from Earth's axis of rotation decreases and, by virtue of conservation of momentum, the speed of rotation should increase. When this current reaches latitude 45°, its distance from Earth's axis of rotation will be 0.707 of its initial value on the equator. Due to this, its speed of rotation near to Earth's axis should increase to 656 m/s. Yet, Earth's surface speed of rotation at latitude 45° is less, and being only 328 m/s. In this case, the warm current should become instable. But since the warm current transfers its stalling momentum through the water layers to the cold one, no significant perturbation of currents takes place. Nevertheless, this form of force impulse transfer through swirl formation observed involves high friction energy losses in swirling water flows.

The hydrodynamic model has shown that Earth participates in water circulation in the ocean by receiving a definite momentum from warm currents and transferring it to cold ones.

And still, the approximate model fails to account for the cause of downwelling of warm currents into cold ones when approaching the polar areas.

Besides, the kinetic energy produced by the difference between the densities of the warm and cold water is clearly insufficient for current transport at a definite speed over thousands of kilometers through layers of immobile water, and for overcoming friction in the swirls being formed.

The situation changes if analysis is conducted using a gas dynamic model.

2.1.2. Gas dynamic circulation model

A priori, it can be asserted that Earth's basic angular momentum occurs in the low and mid-latitudes that receive the bulk of insolation. Indeed, if a huge mass of water continuously evaporates to the atmosphere in the form of high-speed vapor-air flows, the ocean should experience a response, transmitted further to the Earth.

Let us trace the energy conversion path. For this, we will consider several schemes explaining the processes observed.

Let us dissect the Earth along the equator and look at one of the sectors from outside, e.g. the North Pole (Fig. 6). In case of an immobile Earth, vapor flows rise radially from its surface, entrapping therewith the air and heating it.

Each vapor flow (arrow A) imparts its momentum to the Earth. The reaction forces are directed along the radius to Earth's centre. Since the vapor flows are arranged evenly over the spherical surface, the arising force impulses mutually compensate one another.

When the Earth rotates, the case is different. An insignificant lag of the atmosphere's rotational speed with respect to that of the Earth leads to curvature

of the direction of motion of vapor flow A'. The impulse, equal to the momentum acquired by the flow due to ocean's heat energy, has the same direction (Fig. 7). Vector A is the response of this force. Let us decompose vector A to components B and C. It is the force represented by vector C that causes Earth to rotate.

At this phase of the study, we will limit ourselves to examining the processes in the boundary layers.

Laminar layers with an anomalous temperature are located at the very ocean-atmosphere boundary. Here we are interested in a water layer about $5 \cdot 10^{-2}$ m thick, where the temperature drops by 1 to 3 °C towards the phase interface. This drop is caused by the surface layer's heat loss due to radiation to the atmosphere, evaporation and contact heat transfer with air. However, the bulk of heat escapes to the atmosphere by water evaporation.

The thermocline, with a higher water temperature, underlies the thin layer [23 and 24].

The thin laminar layer of the atmosphere, which is in direct contact with the ocean's surface, is also involved in creating Earth's angular momentum. Let us specify only such a thickness of the atmospheric layer, where the temperature difference above the phase interface is the same as that in the surface water layer, i.e. 1 to 3 °C. This assumption rests on the fact that the phase interface cannot be considered strictly fixed. Even in calm weather, the ocean's surface swell crest tops and small splashes move beyond the height corresponding to the thickness of the atmospheric boundary layer selected.

Hence, the total temperature difference, ensuring water evaporation from the ocean's surface, is 2 to 6 °C.

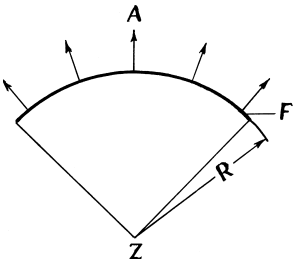

Z — Earth's centre; R — radius; F — section of Earth's surface; A — direction of movement of moist airflows.

Fig. 6. The equatorial section sector of an immobile Earth

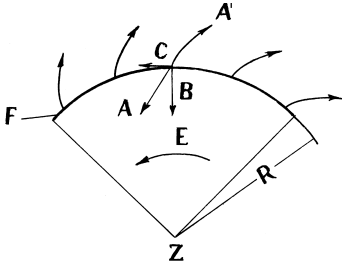

E — direction of Earth's rotation; A' — moist flow's force impulse vector; A — response; B and C — response components.

Fig. 7. The equatorial section sector of rotating Earth

Now, to evaluate the momentum received by the Earth at the atmosphere-ocean interface, we, by right, can use the known triangular cycle. For this, let us consider a system comprising a warm current, for instance, Gulf Stream, and a reverse cold current in the ocean's deep. As the warm current flows northward, part of the water evaporates, and the vapor so formed ascends. A sharp vapor temperature drop per unit altitude can be observed in the thin layers adjacent to the ocean's surface. In the atmosphere's upper layers, vapor condensates and falls as rain to Earth.

This sequence of events is graphically shown on the T–S diagram as a stepwise triangular cycle (Fig. 8). Water evaporation from the ocean's surface layer corresponds to adiabatic processes c_1d_1, c_2d_2, c_3d_3, etc. Let us assume, by convention, that vapor extraction from the atmosphere's thin laminar boundary layer is equivalent to its condensing. After water vapor has condensed and the bulk of cooling water has been displaced with the current flow (processes d_1a_1, d_2a_2, d_3a_3, etc.), water is transported to the heating zone (processes a_1b_1, a_2b_2, a_3b_3, etc.). Finally, lines b_1c_1, b_2c_2, b_3c_3, etc. relate to the process of water heating by solar radiation.

The total area of the triangular cycles of the current's separate sections corresponds to the amount of heat converted to work spent on Earth's rotation acceleration.

The sum of the lengths of vertical sections a_1b_1, a_2b_2, a_3b_3, etc. correlate with Earth's work spent on cold current transport to the equator. Earth's work on overcoming its deceleration due to fallout of earlier evaporated vapor as rain is also to be related to this work. The amount of energy received by Earth in one of the warm current sections is transferred immediately to the section of the cold current that flows in the lower water layers. In essence, Earth acts as a distinct multistage turbine pump, continuously generating and immediately consuming mechanical energy. In so doing, the diameters of the turbine stages decrease from the equator to the poles, and those of the pump, conversely, increase. Thereby, Earth manages to transfer excess heat from the equator to the poles.

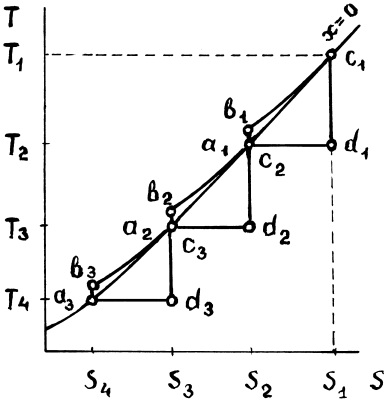

Fig. 8. Stepwise cycle of Earth's flow circuit in the T–S coordinate system

Reaction C, ensuring Earth's rotation (Fig. 7), manifests itself only before the zones of warm water downwelling to the ocean's deep. In itself though, warm water downwelling is caused by the intake effect of submerged parts of continents rotating together with Earth. Thus, for example, the continental platforms of Antarctica's peninsulas act as centrifugal pump vanes that intake water (including that downwelling from the surface) and discharge it in the reverse direction to the equator. In so doing, the bulk of depth water upwells over the continental platform slopes to the surface. Preserving their angular momentum, the water currents expulsed to the surface partially support the circumpolar current formed by Western winds around Antarctica.

The Arctic Ocean floor has about the same effect. Imagine a bowl half filled with water, with the bowl's section slightly increasing with height. Then let us rotate the bowl rapidly about its axis. The water shall also start rotating, rising thereby gradually over the tapering wall and spilling over its edge. The ocean floor acts in the same way by intaking water currents in its central part and discharging them to the equator with its peripheral higher part.

From triangular cycle analysis, we know that a warm current, in replenishing the mass of diminishing cold water, has sufficient momentum for moving from the surface to the ocean's floor rotating central part. The mechanism of action of those parts of Antarctica's continental platform protruding to the equator, and of the Arctic Ocean floor presented here is quite real, if one assumes that rotation of the World Ocean about Earth's axis lags somewhat in the near-polar regions with respect to rotation of the planet per se.

Let us consider Earth's properties as a reaction turbine. From theory, the maximum efficiency of such turbines is known to be achieved when the available temperature difference is divided into several parts. In this case, the steam flow velocity in each stage can be reduced, thereby ensuring minimal flow friction loss on the channels' walls [25 and 26].

Earth successfully resolves this problem by implementing a multistage triangular cycle.

The attainable efficiency of small-diameter nozzles $(3 \text{ to } 5) \cdot 10^{-3}$ m in a boiling liquid-driven reaction turbine is within 64 % [27]. One can imagine a honeycomb arrangement of circulation cells above the surface of warm currents. The rise channels of these cells will then act as reaction turbine nozzles.

The latter fact offers the possibility of making an approximate experimental estimate of the internal efficiency of circulation cells acting on the ocean-atmosphere boundary at 2 to 6 °C temperature drops.

Note that the total effect of cells consists in imparting a certain momentum to Earth, which converts it to an angular momentum. Hence, the experi-

mental model should look as a massive vertical shaft simulating Earth's body, with a mounted thereon reaction turbine (an analog, for example, of Earth's equatorial zone) and a circulation pump (an analog of Antarctica's continental platform). Due to Earth's spherical shape, the turbine diameter should be considerably greater than that of the pump.

Besides, this model can also be considered as a separate stage of the following macrosystem: warm current — Earth — cold current.

The installation has to be fitted also with a heat exchanger for heating the circulating water, and a condenser for condensing steam generated when water boils inside the turbine nozzles.

We will demonstrate that, at temperature superheating of the circulating flow within 2 to 6 °C, the turbine pump shaft will start rotating on its own. In so doing, the turbine-generated energy will be sufficient to drive the circulation pump to intake the cold water downstream the turbine and condenser, and to discharge it via the heat exchanger to the same turbine. Such circulation corresponds to water circulation observed in the ocean.

Besides proving the thermodynamic nature of Earth's rotation, associated with circulation of flows, the model should allow for evaluating the efficiency of flow circuits acting at so small temperature differences.

Basically, a compact evaporator installation with a turbine-driven circulation pump [28] meets the requirements set forth to Earth's experimental model.

Let us consider the results of testing this installation. The external view of the installation is shown in Fig. 9, and its schematic diagram is given in Fig. 10.

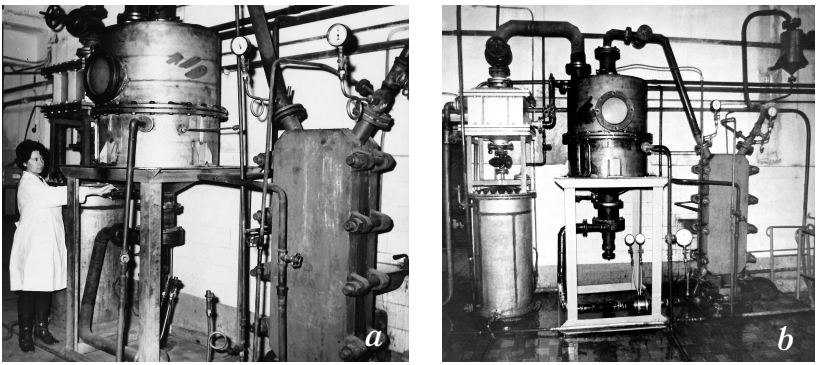

Fig. 9. External view of the evaporator installation:
a — during erection; b — in operating condition

2.2. EVAPORATOR WITH A TURBINE-DRIVEN CIRCULATION PUMP

During evaporator installation operation (Fig. 10), superheated steam from heating chamber 6 flows through a connection pipeline and hollow shaft 3 to the horizontal channels in the Segner wheel, and therefrom to Laval nozzles 4 arranged over the periphery of the channels.

Upon entry to separator 2, the solution boils, and evaporator steam expands to accelerate the steam-solution mixture. The reactive force arising in Laval nozzles starts rotating the vertical shaft to drive circulation pump 5.

From the lower part of the separator, the pump continuously pumps the solution via the connection pipeline and starting pressure relief valve 7 to heating chamber 6; at the same time, evaporator steam is discharged to condenser 1.

The design parameters were changed within the following ranges: turbine diameter — 260, 360, 400 and 560 mm; Laval nozzle critical section diame-

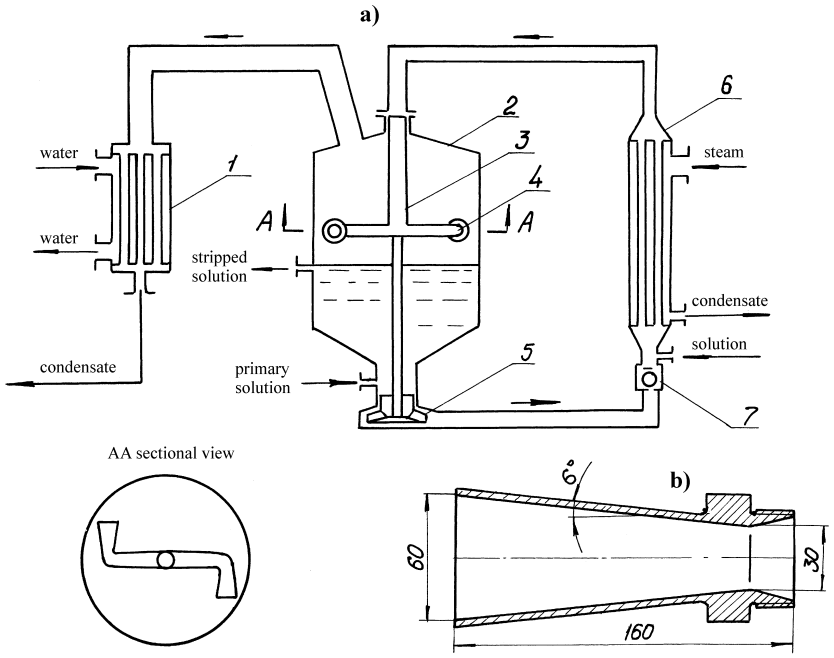

Fig. 10. Schematic diagram of evaporator installation (a) and Laval nozzle (b)

ter — 14, 20, 25, 30 and 35 mm; number of nozzles — 2; diameter of pump vane wheel — 168 and 260 mm; width of pump wheel vane exit section — 12, 15 and 23 mm; separator diameter — 600 and 800 mm; the heating chamber was made of corrugated plates type ПР-0,5Е with 10 channels having an overall section area of $F_k = 0.018$ m^2; and the chamber heat transfer surface was 10 m^2.

When designing the reaction turbine, we took into account the results in works [29 to 31]. The pump was designed by using experimental data [32] to provide an optimal solution flow velocity in the plate-type chamber within 0.3 to 0.5 m/s [33]. In each regime, the installation operated for up to 8 hours, and the process parameters were measured every 30 to 60 minutes. In so doing, we recorded the following parameters: the pressure; the temperature and amount of condensate of primary and evaporated steam; the temperature of circulating liquid at the inlet and outlet of the heating chamber; the liquid flow rate; the flow resistance of the flow circuit and the turbine; and the shaft speed. Peepholes were provided to monitor the flow condition at the hollow shaft inlet and in the Laval nozzles during turbine start-up and shutdown.

The liquid level in the separator was maintained constant by keeping equal the amount of makeup water and evaporated water. The stripped liquid is pure condensate. The limit relative error of measuring the heat transfer rates was ± 7 %. To exclude the effect of depositions, the chamber was periodically flushed with a weak hydrochloric acid solution.

Partial liquid boiling was observed visually at the inlet to the turbine's hollow shaft. Hence, the cycle shown in Fig. 11 was implemented instead of an optimal cycle in the form of a triangle in T—S coordinates. The data of most representative experiments, corresponding to the given cycle, are shown in Figs. 12 and 13, and in Table 1.

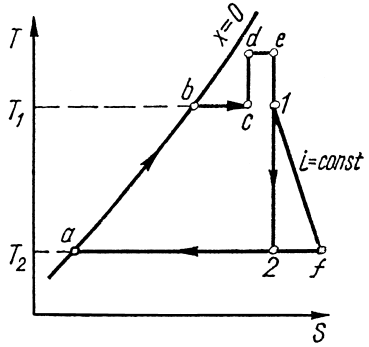

1—2 is the process in the diverging part of the Laval nozzle for an ideal cycle, i.e. without friction energy losses; 1—f is the flow throttling isoenthalpic process; 2—a is steam condensing; a—b and b—c is liquid heating and steam generation; c—d is pressure build-up in the flow in the turbine horizontal channels due to centrifugal force; e—1 is the process in the converging part of the Laval nozzle.

Fig. 11. Evaporating cycle in the T—S coordinate system

Table 1

Experiment No.	Flow temperature, °C		Liquid flow rate, kg/s		Resistance, mm H_2O		Shaft rpm	Turbine capacity, kW	Steam degree of dryness, kg/kg		Flow velocity, m/s	
	Upstream turbine	Downstream turbine	Circulating G	Evaporated $M_\tau \times 10$	Of circuit and turbine	Of turbine			Before nozzle $x \times 10^4$	After nozzle $x \times 10^2$	In nozzle narrow part	Relative at nozzle outlet
1	104.2	100	8.25	1.25	4.9	1.7	500	0.660	7.31	1.495	6.15	29.6
2	106.5	100	8.50	1.53	6.5	3.0	680	0.905	7.14	1.725	5.80	33.4
3	109.0	100	9.10	2.11	7.7	3.9	790	1.142	6.40	2.280	5.75	41.4
4	111.0	100	9.42	2.50	10.1	6.1	940	1.555	6.06	2.600	4.73	52.1
5	115.0	100	9.70	3.28	13.2	8.8	1000	2.090	7.10	3.310	5.06	64.3
6	120.0	100	10.15	4.44	17.0	12.4	1100	2.820	8.40	4.230	5.38	72.1

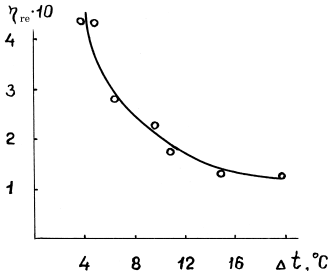

Fig. 12. Turbine effective relative efficiency vs. turbine temperature difference

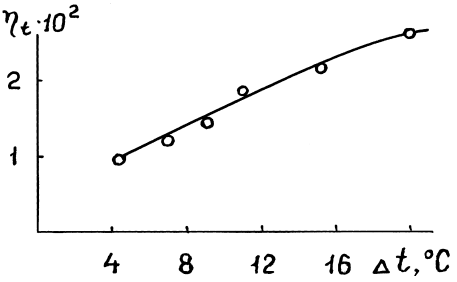

Fig. 13. Flow circuit thermal efficiency vs. turbine temperature difference

Steady circulation is ensured at a turbine diameter that is about twice greater than that of the pump vane wheel. The experimental data presented were obtained when testing a turbine with the diameter of 560 mm, and a pump with the vane wheel of 260 mm diameter. For this combination of geometrical parameters, normal circulation was observed starting with temperature differences of 3 to 4 °C. Should the turbine diameter be small, the temperature difference would have to be increased. Thus, for a turbine with a diameter of 260 mm, and the pump rotor diameter of 168 mm, steady circulation was achieved at the temperature difference of 20 °C in the turbine.

An attempt to decrease the turbine diameter further with respect to the pump impeller diameter leads to flow pulsation and cessation of circulation. Changing the pump wheel vane width does not affect the flow circulation velocity.

Increasing to a certain limit the total area F of the critical sections of Laval nozzles involves an increase in heat transfer intensity. For steady-state circulation, area F should be about 10 times less than the total cross-section F_k of the heating chamber channels.

With account of this, the effect of the thermal load on heat transfer intensity was investigated at $F = 14.12 \cdot 10^{-4}$ m^2. Table 1 shows that a change in the heating chamber temperature difference affects the heat transfer intensity, this being manifested by the liquid starting to boil in the chamber. In the following, the procedure of calculating the efficiency by experimental data is given.

Mixture steam content x_f, at conventional throttling of the flow to the separator, is determined by the expression $x_f = M_\tau/G$. In this case, the mixture enthalpy is $i_f = i' + r_f x_f$.

At an isoenthalpic throttling process i = const, hence $i_1 = i_f$ [7].

The mixture steam content upstream the turbine $x_1 = \frac{i_1 - i'_b}{r_1}$. The flow entropy upstream the turbine $S_1 = S_b + \frac{r_1 x_1}{T_1}$.

At an adiabatic expansion process, equality $S_1 = S_2$ holds. After completion of the adiabatic process, the mixture steam content is

$$x_2 = \frac{S_2 - S'_2}{S''_2 - S'_2}.$$

After completion of adiabatic expansion, the enthalpy of the steam-liquid mixture is

$$i_2 = i' + r_2 x_2 .$$

The thermal efficiency of cycle 2ab1, at reversible steam expansion, is: $\eta_t = \frac{i_1 - i_2}{i_1 - i'_a}$. Measuring the pump's characteristics simplifies the calculation of the turbine's relative effective efficiency.

Power consumed by the pump is found from formula

$$N_P = \frac{G\Delta p}{102\eta_P},$$

where Δp is meters of water column; η_P is the pump efficiency; and the turbine capacity is found from formula

$$N_T = \eta_{r.e} \frac{G(i_1 - i_2)}{1{,}000}.$$

The turbine relative effective efficiency $\eta_{r.e}$ is found from the equality of expressions for N_P and N_T. The calculated values of $\eta_{r.e}$ and η_t, depending on the turbine temperature difference, are shown in Figs. 12 and 13.

The steam-liquid flow resistance of the supply pipeline causes a temperature difference drop by about 3 °C. The resulting thermal efficiency values calculated by experimental data turn out to be lower than those expected are.

Significant losses in the turbine are caused by impact of the steam-liquid jet, exiting one nozzle, against the casing of the other one, and, perhaps, by the metastability effect [27]. The latter is confirmed by weak liquid dispersion at the Laval nozzle outlet. Both negative factors are enhanced with a temperature difference increase, and hence, a rotational speed increase.

Without account of mechanical losses, the thermal efficiency value of an actual cycle is found from the dependence $\eta_{tz} = \eta_{r.e}\eta_t$. Since, with an increase in Δt, the values of η_t increase, and those of $\eta_{r.e}$ decrease, the thermal efficiency η_{tz} of an actual cycle depends weakly on the turbine temperature difference. On the average, for the accepted design scheme of the chamber, turbine and pump, the cycle efficiency $\eta_{tz} = 0.25$ %. This allows for normal operation of the circuit at solution superheating within 3 to 4 °C, which is required for proving the spontaneous rotation of Earth's model at extremely small pressure differences in the circulating working medium.

Analyzing the design of the circuit and turbine points to the possibility of implementing several measures aimed at reducing friction loss, i.e. increasing $\eta_{r.e}$ values.

The following problems were solved when designing and testing the installation: compensating for shaft temperature elongation and the axial force arising during pump operation; excluding vortex formation in the liquid layer above the pump; cooling of packing glands and bearings; and installation start-up. In absence of pressure relief valve 7 (see Fig. 10), heating steam delivery to the heating chamber initiates intensive solution boiling. The secondary steam that appears displaces the liquid partially via the upper pipeline, and partially via the lower pipeline to the separator, this leading to attenuation of the heat transfer process. To provide steady circulation, it is necessary to ensure solution boiling in the critical sections of Laval nozzles.

Providing pressure relief valve 7 in the circuit and feeding the primary mixture with an increased flow rate directly to the heating chamber allows accelerating the turbine to the required speed. As soon as the circulation pump builds up a pressure exceeding that in the chamber, the pressure relief valve opens to pass the flow through the chamber to the turbine. As circulation becomes established, feeding the installation by delivering the solution directly to the heating chamber is terminated.

As evident, the very fact of developing this installation confirms the imperfection of the hydrodynamic model of flow circulation. Thus, in terms of hydrodynamics, locating the turbine at the outlet of the flow circuit rise channel offers only additional resistance. Nevertheless, the installation performs perfectly, allowing to use the gas dynamic model for studying natural processes.

Let us address the legitimacy of using this installation as Earth's model.

First, introducing the natural air environment into the model converts the water boil process to a surface evaporation one.

Further, in oceanology it is conventional to relate thin interface layers to laminar systems, where heat conduction and diffusion affect heat and matter

exchange. This approach, however, is not altogether correct. It has been established that negligible temperature variations, both vertical and horizontal ones, accompanied by changes in the surface tension of water, induce the origination of circulation cells (Marangoni instability). These cells ensure intense water mixing in the interface [34]. Insignificant temperature drops between air layers are also known to cause natural convection of flows [35].

This motion becomes more intense when water vapor enters the circulating flow.

At atmospheric pressure, the volume of a unit mass of water converted to vapor increases by a factor of 1,600. Under these conditions, part of the thermal energy inevitably transforms into the kinetic energy of flows. It is at the ocean-atmosphere interface that chaotic heat motion of molecules in the water surface layer acquires orderliness in the ascending vapor-air flows.

The swell observed on the surface of seas is apparently due to the action of reaction forces occurring in the rise channels of small circulation cells.

For the case being considered, the problem, in essence, consists in a comparative evaluation of the efficiency of the rise channel in one of the cells, and of the efficiency of the nozzles in the circuit that has been tested.

Baseline data for calculating the efficiency of a small cell

Temperature difference, Δt °C 5
Temperature of the lower boundary of the thin layer of water, T_1 K(°C) 301 (28)
Temperature of the upper boundary of the thin layer of atmosphere,
T_2 K(°C).....296 (23)
Hydraulic steam turbine parameters at the temperature difference of Δt, °C 5
η_t = 1.0 %; $\eta_{r.e}$ = 38 %; η_{tz} = 0.38 %

Calculation

Let us determine the thermal efficiency of a circulation cell

$$\eta_t = \frac{T_1 - T_2}{T_1} = \frac{5}{301} = 0.0166.$$

$$\eta_t = 1.66\ \%.$$

Now we shall estimate the internal efficiency value $\eta_{i.e}$.

Since in the cell's rise channel the medium is a single-phase one, friction losses will be considerably lower than those in the turbine nozzle are. But we are considering the cell's rise channel as a nozzle of a reaction turbine. At best, 50 % of mechanical energy obtained will be spent in the jet, and 50 % will be spent with Earth's rotating mass. Hence, in the optimal case, $\eta_{r.e}$ = 50 %. In the worst case, this efficiency cannot be lower than that of the hydraulic steam turbine, i.e. $\eta_{r.e}$ = 38 %.

Whence, the total efficiency is

$$\eta_{tz(1)} = 0.0155 \times 0.5,$$
$$\eta_{tz(2)} = 0.0166 \times 0.38,$$
$$\text{or } 0.63\ \% < \eta_{tz} < 0.83\ \%.$$

Hence, the ocean and the atmosphere, in their thin boundary layers, spend only 0.6 % to 0.8 % of the available thermal energy on rotating the Earth.

Undoubtedly, the evaporator model tested only approximately corresponds to Earth's model. The previous calculation is indicative of this. The key distinction of these two objects, however, consists in that the ocean's mass accounts for only 0.02 % of Earth's mass, whereas the mass of water in the evaporator flow circuit even slightly exceeds the turbopump mass. The distinction noted in the mass ratios, however, affects only the inertial properties of the objects being compared. Thus, if only one to two minutes are required to accelerate a turbopump from 500 to 1,100 rpm, several million years will be needed to accelerate Earth's rotation by several revolutions a year.

Hence, tests of the compact evaporator allow to claim that circulation of waters in the World Ocean involves Earth's centrifugal field. This involvement is natural and it occurs only at a certain combination of system parameters coordinated with Earth's preliminary spin.

From these experiments, it also follows that, at small temperature differences, the efficiency of converting ocean thermal energy to the kinetic energy of currents does not exceed one per cent.

Note that the circulation device — the turbopump — has bilateral and rotational symmetry. Earth's flow circuit also possesses the same properties.

To examine the effectiveness of Earth's flow circuit as a thermal machine, let us consider the hydrodynamics of Jupiter's currents.

2.3. FEATURES OF JUPITER'S ROTATION

The necessary condition of a planet's rotation is the presence, in its outer shell, of a substance (working medium) capable of changing its volume during evaporation and condensation. On Earth, such a substance is water, and on Jupiter, it is hydrogen. The heat sources are the Sun and the planet's deep, and the cooler is the surrounding space.

Heat efflux from the equatorial zone of planets to the poles is ensured by a system comprising three macroelements, which exchange a certain momentum, viz. a warm current, the planet's body and a cold current.

Though it is difficult to distinguish warm currents under a thick layer of clouds, upwelling of cold currents close to the equator can be detected by spots formed in the atmosphere. The cause of this is that gaseous hydrogen, which comprises the atmosphere, condenses above the areas of efflux of supercooled liquid hydrogen to the ocean's surface. The fact that the biggest spot (the so-called "Red spot") is found in the southern hemisphere, whereas only several small spots are located in the northern one, can be explained by the polar asymmetry of the heat drain.

Jupiter's South Pole, similar to Earth's South Pole, radiates more energy to space than the North Pole does, this being the cause of more intense current circulation in the southern hemisphere.

The principle of current distribution on Jupiter is an original one. Both solar radiation energy and the depth heat of the planet itself are delivered to the equatorial zone comparatively uniformly. At the same time, cold currents upwell to the equator in separate limited areas. To heat supercooled hydrogen, its currents should be distributed uniformly over the planet's surface. This problem is solved on Jupiter more successfully than on Earth where cold currents, e.g. in the Northern Hemisphere, are isolated from one another by continents.

Cold liquid hydrogen currents (ropes), in being dragged by the planet, as if roll over the denser underlying layers. Such a current flow regime causes the "ropes" to rotate about their axes in a direction opposite to that of the planet's rotation. Concurrently, the "ropes" lag behind the rotation of the planet itself in their movement around the planet's axis. It is precisely this phenomenon that causes spreading of supercooled polar hydrogen among the layers of comparatively warm equatorial hydrogen.

In some time, after which Jupiter's South Pole starts facing the Sun, the Red spot's profile should diminish because of a change in the balance of heat influx and drain in this part of the planet. The heat received by the cold current in Jupiter's depth turns out to be sufficient for evolution of dissolved gases, having a reddish hue, from the supercooled liquid hydrogen. The significant heat flux from the depth, low hydrogen density and greater gravity make Jupiter rotate faster as compared to Earth. The obviousness of this fact can be traced by the triangular cycle, taking into account that hydrogen boiling occurs at the depth of several hundred meters.

Note

We would not err much if the same thermodynamic effects accounted for rotation of celestial bodies, possessing a gas-plasma or gas-liquid shell.

In this case, the cause of spots observed on the Sun is near-equator upwelling of colder plasma flows from the poles.

CONCLUSIONS

Let us summarize the studies presented in this section. Earth, in receiving solar radiation energy, is unstable with respect to forces causing it to rotate about its axis. These forces arise spontaneously due to heat redistribution in the atmosphere and the ocean. The mandatory condition of force manifestation is the presence of three macroelements, which exchange a certain momentum, viz. a warm evaporating water current moving poleward from the equator, the planet's body, and a cold current moving from the pole to the equator.

For analysis, the flows are divided into separate stages. The efficiency of one such stage, calculated for the temperature gradient in the thin atmosphere-ocean boundary layers, does not exceed one percent.

It is also clear that this process has a natural character. But, as distinct from the previous case of natural circulation, where the gravitational field ensures delivery of the bulk of cold water to the heating zone, here the governing factor is Earth's centrifugal field. This allows calling this type of circulation as the rotational effect.

Since rotational instability occurs when the system has acquired a definite combination of parameters, and after Earth has been prespinned, the effect considered can be also related to the category of spontaneous ones.

Comparative thermodynamic analysis shows that Jupiter's high speed of rotation is associated with a significant gravitational field, low density of gaseous and liquid hydrogen, and delivery of the bulk of heat from the planet's depth.

CHAPTER 3

THERMODYNAMICS OF THE ATMOSPHERE

Let us study the planet's resistance to secular change of the climate. Besides, we will trace the trends in climate changes over the past millennia.

As mentioned above, the ocean's surface layers at the equator are heated to 27 to 29 °C. Water vapor condenses in the atmosphere at 0 °C. Hence, the available temperature difference at the equator is about 27 to 29 °C, and in the midlatitudes, this value drops to 15 to 20 °C.

In their boundary layer, the ocean and the atmosphere spend about a fifth part of the available temperature difference on Earth's rotation, the atmosphere accounting for the remaining part.

Hence, the bulk of heat energy, capable of converting rapidly to kinetic energy, is found in the atmosphere.

As the American meteorologist, Joan S. Malcus wrote, "Water vapor is the key "fuel" of the atmosphere". At least in its lower layers, namely in evaporation processes, should one look for the cause of air motion, i.e. the wind. The wind, in turn, affects the sea by transferring the mechanical energy directly thereto. And this energy is the major cause of emergence of universal systems of surface ocean currents and sea waves [22].

As distinct from the ocean, the atmosphere's lower layers heat up to facilitate natural circulation of flows. In low latitudes, stable circulation cells (Hadley cells) originate, and in the midlatitudes, weak circulation cells (Ferrel cells) appear. Easterly winds in the equatorial zone and westerly ones in the midlatitudes augment zonal circulation. Different large-scale turbulent formations of the cyclone, anticyclone and wave-structure types in zonal flows ensure the necessary heat transfer and angular momentum [36–38].

At the same time, several aspects of the general circulation of the atmosphere have not found an adequate theoretical explanation. In particular, the conditions of origination and dissipation of kinetic energy have in no way been linked to a change in Earth's rotational speed. Besides, the physical model of

processes was developed without accounting for the atmosphere's condition in the Ice Ages. Without reconstructing the climatic conditions in the past, it is impossible to understand the weather and climatic changes observed presently.

Let us consider the key zones, where the angular momentums originate at present, and establish the regularities of their transfer to Earth by the atmosphere. The same operations will be performed for glaciation periods, with a refinement of how Earth's rotational speed changed in that case.

Let us assume that moist air flows, accelerating upward, impart to the Earth a definite momentum.

Since, as mentioned earlier, the atmosphere somewhat lags with respect to Earth's rotation, the air flows ascend from the ocean's surface over a curved path. In so doing, the flows' sections increase with height. The shape of each profile resembles that of the curved Laval nozzle. The force impulse vector can be decomposed into components similar to that for the vector in the atmosphere-ocean boundary layer (Fig. 7). As a result, the horizontal component of the impulse reaction isolated by us should facilitate Earth's rotation. At the same time, this scheme of energy conversions holds only for calm conditions, not disturbed by any atmospheric perturbations. With appearance of horizontal, or vortex-type airflows, the slope of vertical flows should change to either side. If they incline in opposition to Earth's rotation, the vertical warm airflow accelerates Earth's rotation, otherwise it retards it.

3.1. GAS DYNAMICS OF VERTICAL VAPOR-AIR FLOW IN THE EQUATORIAL ZONE

Let us consider air distribution in low latitudes. Air, in settling in the high-pressure zone, returns in part to the equatorial belt in the form of trade winds — the most steady winds on Earth. Trade winds blow equatorward from the northeast in the Northern Hemisphere, and from the southeast in the Southern Hemisphere.

The time of trade winds' blowing equatorward from latitude 30° is about three weeks; the flow velocity is 5 to 8 m/s, and the meridional deflection speed is 2 m/s. During this time, the trade winds heat up and become moisture-saturated. Major water vapor condensation occurs in the equatorial trough, extending within 0 to 20°N. Convergence of Northern Hemisphere trade winds with those in the Southern Hemisphere enhance vertical airflow. Water vapor condensation causes the formation of huge towers of cumulus rising to 10 to 11 km, and sometimes even to 15 km. These towers are frequently

called heat ones because of the great amount of kinetic energy generated during water vapor condensation. The amount of this energy has been estimated to exceed by far the amount of kinetic energy of all winds and airflows on the planet [21]. The direction of trade winds ensures, during their meeting, an inclination of heat towers in opposition to Earth's direction of rotation. In this case, the horizontal components of the reactive force impulse, created by the towers, impart to the Earth an additional angular momentum.

Hence, it is in the equatorial zone that Earth acquires its major angular momentum.

In this case, the thermal efficiency of rise channels with a height from the thin atmosphere's layer boundary to the cloud formation zone increases to 7.8 %. The internal efficiency falls to some extent because the height of the riser channel is significant, and the vapor-air flow velocity therein is high. Both factors lead to appreciable friction energy losses.

The towers convert not only the heat of the surface layer water in the trough zone, but also the heat of water vapor attracted to the equator from adjacent latitudes. As distinct to the thin boundary layer, for which calculations were done to the triangular diagram, here the calculations are done to typical heat diagrams applied to steam turbines (see the following Chapter).

Nevertheless, the degree of involvement of heat towers in increasing Earth's angular momentum is determined by the hydrodynamic situation created by horizontal airflows abutting the trough zone. Therefore, a qualified estimate of the amount of energy received by Earth requires additional studies in the hydrodynamics of flows in Earth's equatorial zone.

3.2. GAS DYNAMICS OF HORIZONTAL FLOWS IN A MOUNTAIN RANGE SYSTEM

The case is different for that part of heat flows, which is carried by air masses across the midlatitudes to the Arctic and Antarctica. Let us distinguish that season when warm southwestern and western winds persist in the midlatitudes of the Northern Hemisphere. At this, both warm airflows and warm water currents move ahead of Earth's rotation, and deflect northward due to Coriolis force.

Let us assume that warm air currents flow from the Pacific Ocean to the North-American continent. We shall trace their interaction with the Cordilleras Mountain Range.

When the airflow cools in the Range foothills, the water vapor in the flow condenses. At this instance, air pressure in the flow falls, and the flow develops

a high velocity. Upon entering the space between the mountains, the flow decelerates. Instant deceleration causes conversion of flow kinetic energy to potential energy. This makes pressure build up on the glaciers' surfaces. It significantly exceeds the pressure of air in the zone of flow formation above the Pacific Ocean. Cold air rises above the mountains and then flows back to the ocean.

Suppose that moist air from the Atlantic Ocean flows to the opposite side of the continent. As mentioned earlier, its bulk flows in the northwestern direction, but some of it flows west to the Cordilleras Range. These airflows cover significant distances over plains, where, in cooling, they lose the bulk of their moisture. As a result, the air pressure developed on the eastern slopes turns out to be considerably lower than the flow deceleration pressure on the western slopes of the Range. This gives rise to an angular momentum accelerating Earth's rotation (Fig. 14).

Let us explain the above by several examples. A gas jet, in colliding with an obstacle, converts its kinetic energy to potential energy. In so doing, the gas pressure restored at the obstacle equals maximum 70 to 80 % of the initial pressure (Fig. 15) [39].

The pattern changes when a steam flow cooled by water is retarded. Steam condensation makes the steam-liquid mixture speed increase, which, in the jets' meeting with an obstacle, or closed space, ensures an increase in mixture pressure to a level significantly exceeding the primary steam pressure level (Fig.16).

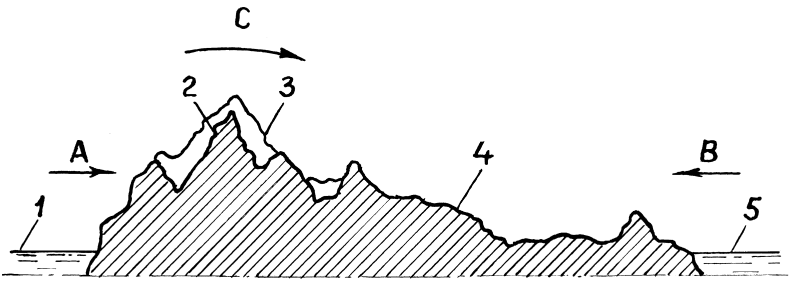

1 — Pacific Ocean; 2 — Cordilleras peaks; 3 — glacier; 4 — continent; 5 — Atlantic Ocean; A — eastward moist airflow; B — westward moist airflow; C — direction of angular momentum.

Fig. 14. Midlatitude section of the North-American continent

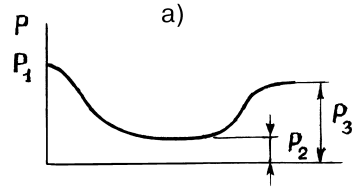

P_1 is the air initial pressure; P_2 is the pressure of a jet exiting the nozzle; P_3 is the pressure of a retarded jet over a flat wall.

Fig. 15a. Pressure change over the length of an air jet

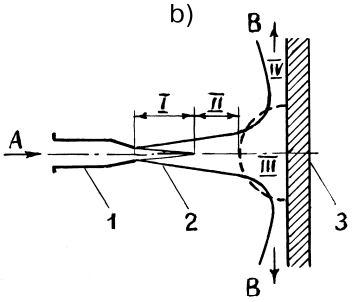

1 – air nozzle; 2 – jet; 3 – flat wall; A – air inlet; B – retarded outflow. Flow areas: I – initial section; II – basic section; III – flow deflection zone; IV – steady-state radial flow zone.

Fig. 15b. Scheme of axisymmetric jet impingement against a flat wall

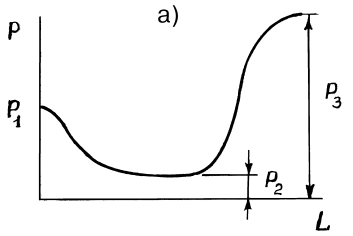

P_1 is steam pressure; P_2 is pressure of a mixed flow in the nozzle's cylindrical section; P_3 is retarded flow pressure at the diffuser outlet.

Fig. 16a. Pressure change over the flowing part length of a steam-water injector

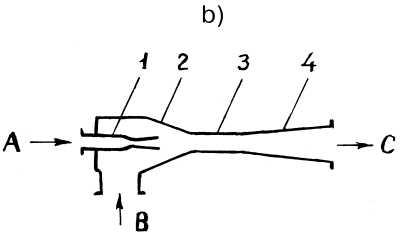

1 – steam nozzle; 2 – cold water chamber; 3 – cylindrical section; 4 – diffuser; A – water steam inlet; B – cold-water inlet; C – retarded flow outlet.

Fig. 16b. Scheme of a steam-water injector with a cylindrical mixing chamber

Let us consider this process with reference to thermodynamic diagrams. As cycle analysis in the $i-S$ coordinate system shows, the pressure of a mixed flow can be higher than the steam pressure only if the straight line of an ideal condensation process, connecting the points of the initial state of interacting media, lies in the region of high isobars, as compared to isobars of their initial state (Fig. 17) [40].

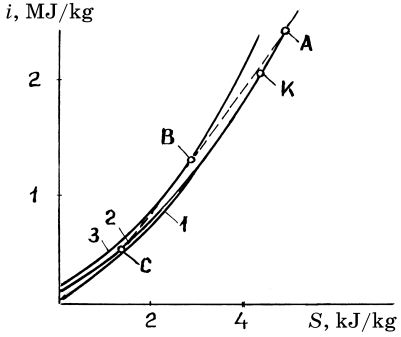

1 — boundary curve (x = 0); 2 and 3 — low and high-pressure isobars; A — saturated steam at low pressure (x = 1); C — cold water at low pressure; K — critical point; B — tangency point of the line of an ideal reversible condensation process, during flow mixing, with the high-pressure isobar; the dashed line is the reversible mixing line

Fig. 17. Compression cycle of steam jet reversible condensation when interacting with cold water

We employed a steam-water injector to pump cold water at atmospheric pressure to a high-pressure hydrogen reactor by using a steam jet taken from the same reactor [41]. We also have gained an extensive background in operating such devices in boilers of different types [42]. The injector's heat energy-to-kinetic energy conversion factor does not exceed 0.5 to 0.6 %. Since the temperature level of natural steam is lower than that of industrial process steam, at equal temperature differentials the natural injector heat efficiency is considerably higher than that of a commercial one. However, on the other hand, the density of natural steam is significantly lower than that of industrial process steam, which, as we have come to know, reduces the internal efficiency value. As a result, the total efficiency values of both types of injectors are approximately equal. In commercial injectors, the working medium is water steam, and the compression medium is water. Water, as known, does not change its volume during compression.

In natural injectors, the working medium is also water vapor, and the compression medium is air. Air is an elastic body that changes its volume during compression.

This leads to different performance of natural and commercial injectors.

If, for example, transport injectors are capable of increasing water pressure by 10 to 15-fold, natural injectors, at the same efficiency, create an air pressure in mountains, which exceeds the pressure above the ocean only by 1.5 to 2 times.

One can judge the possible retarding pressure level by the velocities of movement of hurricanes and typhoons governed by the same physical principle. Dynamic structures observed in the atmosphere, for example, cyclones (Fig. 18), occur due to the joint action of gravitational, rotational and compression effects.

Based on experience in operating commercial injectors, it follows that the natural compression effect occurs only at a significant temperature difference between the moist airflow and the glacier.

Clearly, the maximum possible temperature difference will be observed for glaciers located in the low, and partly, midlatitudes.

Another, and perhaps, major feature of a natural injector is that the compression effect occurs unexpectedly when the system acquires a certain combination of parameters, and just as suddenly disappears when it loses this combination.

From the above calculations it follows that the Cordilleras Mountain Range, extending from North to South over the Americas to 18,000 kilometers, acts as a highly efficient turbine vane accelerating Earth's rotation.

Greenland makes a major contribution to this process in that its glaciers condense the moisture of warm air currents flowing from the Mexican Gulf and the Caribbean Sea over the territory of the Eastern States of the U.S.A.

Let us proceed to analyze how the atmosphere in the zones of Eurasian and African mountain ranges affects Earth's rotational speed. As seen, both continents are flanked with mountains in their southern and midlatitudes. This creates favorable conditions for occurrence of compression effects and their mutual compensation.

This general pattern, however, has one essential deviation. Easterlies are known to prevail near the equator, but over the Sahara Desert — Himalayan

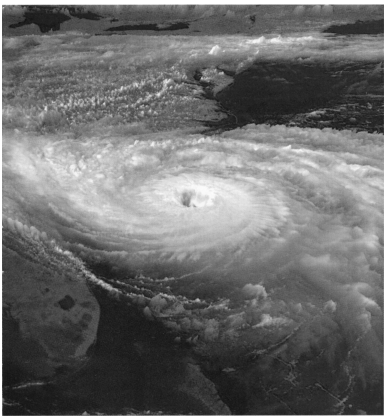

Fig. 18. Cyclone (photo by NASA)

Mountains area, steady westerlies are observed, especially in the spring. Air currents, being heated over Africa's sands, flow eastward and, having passed over the Red and Arabian Seas, meet the huge mountain range on the Hindustan Peninsula. In flowing over the seas, the air currents absorb moisture.

Let us examine this process by example of water evaporation in an airflow. We will take the process in film evaporators as a baseline one. We assume that water is entrained upwards as a film by the high-velocity gas flow in the vertical tube (Fig. 19). Let us investigate the regularities of this process under extreme conditions when the air temperature rises to 150 to 200 °C, and the water temperature rises to 70 to 75 °C. It turned out that the airflow with the velocity of 20 to 35 m/s in the tube dia. $18.1 \cdot 10^{-3}$ m, reduces its temperature to 45 to 47 °C as early as over the length of 1.2 m. A similar effect occurs with the water film moving upwards over the tube wall with the velocity of 0.2 to 0.3 m/s. The air humidity increases from 1 to 2 % to 100 % [43].

As evident, both airflow heat and water heat are spent on evaporation.

It follows herefrom that westerlies expend, on their saturation with moisture, both their own heat received above the Sahara Desert, and the heat of seas over which they blow. As a result, the winds carry a huge amount of water. The Himalayan foothills area is known for the most intensive and prolonged rainfalls on Earth. Hence, this is exactly the area where the powerful angular momentum originates to be imparted to the Earth by the atmosphere.

To close the circulation cell, the cooled airflow, having given up its moisture to the glaciers, has to ascend over the range slopes, and retreat to Africa.

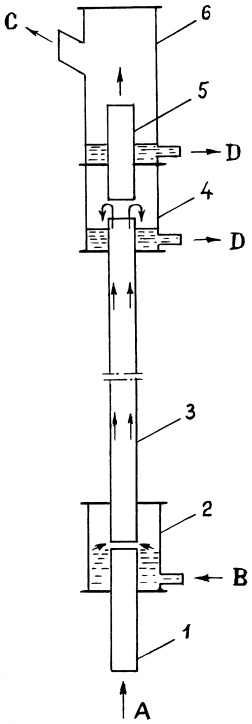

A is the dry air inlet; B is the water inlet; C is the moist air outlet; D is the water outlet; 1 — tube inlet section; 2 — water vessel; 3 — working tube; 4 — separator; 5 — tube baffle section; 6 — additional separator.

Fig. 19. Scheme of a device for investigating heat-and-mass transfer between a hot air flow and an ascending warm water film

The angular momentum of such magnitude cannot occur at the mountain wind load from the Pacific Ocean. The point is that the ocean and atmosphere possess a water evaporation self-regulation capacity. As soon as the intensity of the Sun's radiation energy increases, followed by an increase in evaporation, clouds appear over the ocean. These clouds reflect the bulk of energy inflow, and water evaporation decreases again.

As to the African desert, the skies above it are always clear. One might say that Sahara's heat rotates the Earth.

A quantitative estimate of the angular momentum requires comprehensive data on the airflow velocity and its humidity; the temperature conditions in the atmosphere and ocean; the values of the area and volume of glaciers; the size of the space between the range mountains; the seasonal climate changes; and the inertia properties of atmosphere's and Earth's masses.

Considering the latter two parameters, the atmosphere's dynamic capabilities are noted to be rather limited because its mass is less than 0.0001 percent of that of Earth's one. Moreover, the atmosphere's outer side is contiguous with space, and therefore, in imparting the angular momentum to Earth, it, actually, has nothing to "rest upon".

However, we should keep in mind that the atmosphere is 6,400 kilometers away from the centre of the Earth. At such radius of action, the forces developed by high-speed moist airflows in mountains create a significant angular momentum.

3.3. THE ATMOSPHERE IN COOLING AND WARMING PERIODS

The impact of atmospheric heat processes on Earth's rotational speed can be estimated indirectly by the periods of origination and disappearing of glaciers.

With growth of surface areas and volumes of glaciers, in the near-terrestrial layer there arise hurricane winds, and compression and rotational effects come into being. Over several million years, the combined effort of the Ocean and the atmosphere accelerated the Earth to the maximum possible rotational speed. Intense warm currents flow poleward from the equatorial zone, the atmosphere's chemical composition being changed at the same time. Up to 1.5 m^3 of carbon dioxide are known to be dissolved in one cubic meter of seawater at 4 °C [44]. The content of carbon dioxide in the World Ocean is estimated by experts to be 50 times of that in the atmosphere [45]. Water, drawn from the ocean to form ice sheets, releases its carbon dioxide to the atmo-

sphere. Influx of additional heat with water currents, and enhancement of the greenhouse effect cause melting of Arctic and Antarctic ice. Thawing starts on continents in the midlatitudes, and the ice sheets gradually disappear. Hurricane winds abate with concurrent disappearance of the compression effect, i.e. the cause that initiates Earth's rotational acceleration.

Meanwhile, the Earth continues to rotate by inertia for some time with the previous speed, thereby ensuring a mild climate over its entire surface. Excess carbon dioxide in the atmosphere stimulates biosphere development.

However, current friction in the ocean and atmosphere gradually reduces Earth's rotational speed; and warm currents abate to cause a concurrent abatement of the rotational effect.

Cooling starts in the midlatitudes. The cold waters of oceans intensively absorb atmospheric carbon dioxide, and the greenhouse effect abates. Glaciers, as precursors of the Ice Age, originate in the mountains, and hurricane winds again attack the highest mountain ranges. The compression effect appears and the rotational one intensifies its effect. The rate of propagation of ice sheets sharply increases, Earth's axial rotational motion starts accelerating, and the planet enters its climatic cycle again.

Information on deviation of Earth's rotational speed from a constant value can be obtained from paleontological data by counting the number of days in a year and in a month during the geological past. Such counting is carried out by examining the section cuts of Devonian corals. These corals have daily growth rings similar to the annual rings of trees. Besides, in corals, daily growth rings are superimposed on monthly and annual growth nodes. Counting these rings made it possible to find that, during the period of emergence of tropical vegetation in the Antarctica and on the Spitsbergen archipelago in the Arctic, Earth's rotational speed was 400 revolutions per year. The frequent change of days and nights also favored more even distribution of heat over the Earth. The Devonian period is away from the present one by 400 to 500 million years [46 and 47].

Glaciation occurred at intervals of about 150 million years. Orogeny periods demonstrate a certain correlation with glaciation periods [48 and 49]. Affecting the climate change intervals, orogeny, nevertheless, cannot stop them. Hence, glaciation is an irreversible process. The fact that Earth's rotational speed was high in primordial times leads to several evident consequences within the framework of the theory developed here.

Thus, a separate, sufficiently massive mountain ridge that has emerged anew on any continent, can change the wind rose, and initiate glacier growth. Naturally, as this occurs, the compression effect emerges. If the action of this effect is in opposition to the direction of Earth's rotation, the Earth shall decel-

erate during a rather short geological period, this leading to Earth's losing the gyroscopic effect.

Under the effect of the Moon and Sun, Earth's equatorial plane, tilted presently at 23.5° to the ecliptic, shall turn and occupy a position coinciding with the Sun's orbital plane. It is this effect that caused significant displacement of Earth's poles in prehistoric times. Data on poles' displacement has been obtained by paleomagnetic measurements.

The origin of floods and of the Deluge also becomes clear. When Earth's rotation decelerates, the ocean shall continue moving by inertia with the same speed for a while. As a result, Europe and the Middle East, for example, will sink into the ocean' deep, and the sea should recede from China's shores.

The importance of predicting so catastrophic events depends entirely on interpreting the laws of orogeny. The thermodynamics of the lithosphere, presented in Part II of this book, will clarify the pattern of terrestrial processes in many respects. Current data on Earth's rotational speed, however, are rather contradictory, and, besides, the bulk of these data are limited to historical time. Earth's rotation has been established to be irregular. This irregularity includes the secular deceleration of Earth's rotation (the days become longer by 1 to 2 ms per century), small seasonal variations of rotational speed (Earth's rotation is the fastest in August, and the slowest in March), and, finally, anomalous stepwise rotational speed variations (exceeding secular variations by an order).

Among the causes that initiate poles' oscillation and Earth's irregular rotation, the following can be mentioned: seasonal displacement of air masses, movement of continents, glacier thawing, Earth's elastic properties, and convective motion in Earth's liquid core.

It is believed that, over the past several millennia, secular variations of Earth's rotational speed were caused by tidal friction, but even here, angular momentum variations (assumed to be associated with sea level changes) play an essential role.

Recently, the magnitude of tidal forces arising due to the affect of the Sun and Moon is being evaluated by perturbations in the motion of Earth's artificial satellites [50 and 51].

In being oriented only to historical time data, and neglecting thermodynamic methods of research in natural processes, the authors of the works cited failed to unveil the causes of dramatic climatic changes in prehistoric times. The cause of stepwise changes in Earth's rotational speed has not been explained satisfactorily as well.

Nevertheless, observation data presented in references [50 and 51] are extremely important for predicting future changes in Earth's climate. From

these data is follows that, presently, the rhythms of glaciation and warming find no manifestation in the variations of Earth's rotational speed, as was the case in prehistoric times. Therefore, irreversible changes are occurring on Earth.

Let us point to two such changes.

3.4. CAUSES OF CONTRACTION OF GLACIATION PERIODS

Let us examine the first cause, viz. ocean's behavior in geological time.

The coastline that separates land and sea changes dramatically. It changes depending on whether the amount of water in the ocean decreases when continental ice sheets grow, or, conversely, increases when glaciers thaw (Fig. 20) [52]. As evident, over many hundreds of millions of years, the intervals of origination and decay of glaciers changed little, but the ultimate level of

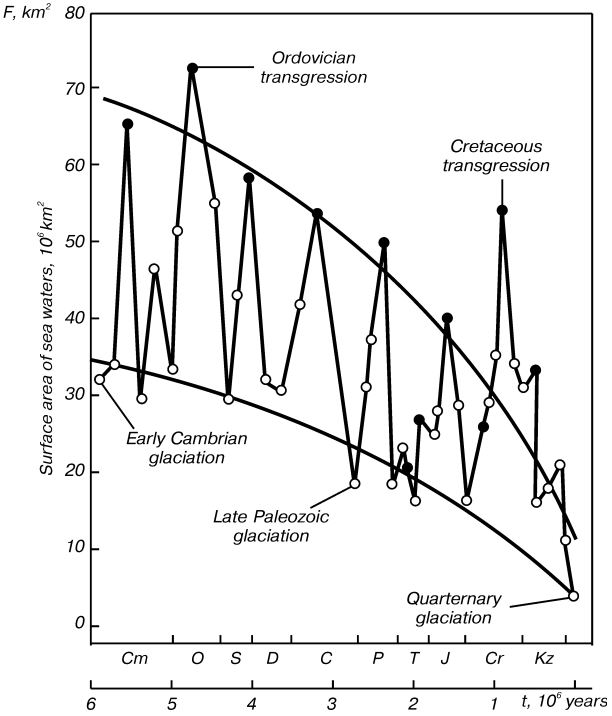

Fig. 20. Curve of dewatering of continents during Phanerozoe

water in the oceans decreased from cycle to cycle. This leads to impairment of water circulation in the oceans, and, consequently, to a decrease in the angular momentum imparted to Earth by the ocean due to the rotational effect. As a result, Earth's axial rotation should decelerate.

The second cause is associated with movement of continents. After Africa had abutted on Asia, in the conventional energy exchange structure "ocean-atmosphere-mountains" a new component "desert-atmosphere-ocean-mountains" appeared. This component sharply increased the angular momentum imparted by the atmosphere to the Earth due to action of the compression effect, which, as a result, should have accelerated Earth's rotation.

Abatement of the rotational effect and intensification of the compression one brought the system to a steady state with anomalous stepwise changes in Earth's rotational speed during the year. Apparently, the same event contracted glaciation periods from dozens of millions of years to dozens of thousands.

3.5. FEATURES OF MARS' ROTATION

Oscillation of mechanical systems is known to occur both near to steady equilibrium positions and near to steady motions. In describing a concrete motion of a mechanical system, one inevitably faces the issue of acting forces. Thus, in line with the principles established herein, a planet having a gas-liquid shell should rotate about its axis under the effect of rotational forces.

The same thermodynamic principles indicate that the rotational speed of a planet with a gas-liquid shell and mountain ranges should fluctuate about a constant value under the effect of compression forces.

As analysis of Earth's and Jupiter's rotation has shown, there is no challenge in determining the values of forces acting in both cases according to the technique suggested.

Therefore, having data on the intensity of energy sources, the planet's mass and the properties of the medium constituting the atmosphere and ocean, we can appraise the rotational speed of a celestial body. Naturally, the opposite statement is true, viz. one can infer on the presence of a gas-liquid shell, and on the intensity of energy sources harnessed by the planet for rotation, by the speed of its rotation.

Let us put to test the validity of this statement in respect to some planets and their satellites. Since the Moon has synchronized its axial rotation with Earth, and Mercury has done so in respect to the Sun, it is possible, even without investigating these celestial bodies, to suggest they have no gas-liquid

shell. Venus is known to have a heavy gas shell. But this does not relieve the planet from synchronizing its rotation with Earth. Venus rotates once about its axis in 243 Earth's days.

At the same time, Mars' rotational speed differs but slightly from that of Earth. Mars presently, however, has no gas-liquid shell, and the atmospheric pressure on its surface is within 0.006 atm. Nevertheless, from the moment of origination of the Solar system and to date, Mars failed to synchronize its rotation with the motion of the closest planets.

It is reasonable to suggest that Mars, at the early stage of its development, had an ocean and an atmosphere denser than at present. The presence of a gas-liquid shell, however, in no way implies that the planet should rotate at high speed. It is necessary to identify an energy source that maintains this rotation.

The conditions of formation of the planet considered apparently differed little from terrestrial ones. Moreover, its mass is one-tenth of Earth's. Due to this, Mars would not be expected to supply a considerable amount of energy from its depth. On the other hand, the density of solar radiation on Mars is one-third of Earth's. This energy is insufficient for Mars even to thaw the ice caps on its poles.

In this connection, one can conclude that in young Mars' sky there was one more star that supplied it with energy sufficient for rotation.

Of Mar's closest neighbors, Jupiter suits this role best. It is not improbable that, at the same time when Mars had an ocean and a denser atmosphere, Jupiter was a star.

The total density of the energy flux received by Mars at that time differed but slightly from the density of the solar energy flux received presently by Earth.

The presence of mountains on Mars caused pulsations of its rotational speed.

With extinction of Jupiter as a star, Mars' ocean transformed into glaciers. The process of formation of ice sheets occurred, apparently, over a short time interval, making it impossible for atmospheric and oceanic currents' friction to reduce Mars' rotational speed.

It is worth mentioning that Earth, in having received an additional amount of radiation energy from Jupiter, also rotated much faster than it presently does.

A direct indication to Jupiter's being a star implies the necessity of in-depth analysis of the initial conditions of formation of the Solar system.

CONCLUSIONS

Let us summarize the problem considered here. The process of Earth's rotation is unsteady with respect to the action of mass forces arising during redistribution of heat in the atmosphere and ocean. This unsteadiness is manifested by a change in Earth's rotational speed, which, ultimately, leads to secular climate variations. Among the mass forces, the most significant ones are those of the compression effect. This effect appears due to retarding of high-speed moisture-saturated airflows in mountains.

Spontaneous appearance of the compression effect causes stepwise changes in Earth's rotational speed during the year.

The ocean contributes to accelerating Earth's rotation by water evaporation from the entire surface of low and midlatitudes, whereas the atmosphere affects this process locally, depending on the sites of heat sources and the location of mountains. The atmosphere transmits the bulk of mechanical energy to Earth in the equatorial zone as well as to regions with mountain ranges, in particular, the Cordilleras and the Himalayas. Earth receives the remaining part due to its surface flow friction at seasonal redistribution of air masses. And only during cooling periods, the momentum imparted by the atmosphere to the Earth, increases pro rata with an increase in temperature differences and the area of glaciers. The atmosphere's basic "fuel" is water vapor.

Earth spends the angular momentum received on driving cold water and air currents poleward from the equator.

Orogeny is capable of altering the direction of the compression effect, this being associated, as a rule, with a change in the tilt of Earth's axis of rotation. This leads to catastrophic events, such as glaciation, earthquakes and flooding.

CHAPTER 4

OCEAN THERMAL ENERGY CONVERSION PLANTS

In the previous section, we evaluated the effectiveness of the action of the terrestrial globe as a device that converts the heat of the ocean and atmosphere to work spent on circulation of flows. According to the established mechanism, the compression effect ensures first a slight "spin-up" of the Earth. Then the rotational effect comes into action and, in comparatively short time, brings the Earth to a rotational speed required by the heat balance.

In so doing, the rotational effect is insensitive to the planet's direction of rotation. The Earth is accelerated in the direction, in which the initial spin forces had acted.

Both effects occur only under dynamic conditions, i.e. connected with influx and outflow of heat during current flow.

A feature of the system considered is that the reaction occurring due to evaporation and condensation of water, imparts just as much mechanical energy to the Earth as it needs for maintaining a constant axial rotational speed.

This statement is based on the fact that, under current conditions, no overheating of Earth is observed. Hence, the Earth returns all the solar radiation energy received to space. Due to the same reason, Earth also cannot accumulate mechanical energy. The slight variation of Earth's rotational speed is an evidence of this.

Earth's behavior is obviously extremely sensitive to energy influx from the Sun and its outflow to space.

Hence, it becomes clear why orogeny has such a dramatic impact on Earth's climate variations. Besides orogeny as a driving factor, Earth's rotational speed can change due to volcano eruptions and falling of asteroids. In the first case, a layer of soaring ash particles is formed in the atmosphere, which reflects solar rays. In the second case, cold water upwells from the ocean's deep to the surface. Both effects have a prolonged disturbing influence on the planet's heat balance.

The natural phenomena mentioned can be predicted, but not prevented. The technological recovery of energy from the ocean considered here is another case.

The ultimate objective of our study, as mentioned earlier, is obtaining data for designing OTEC plants.

To achieve this objective, we have to solve several challenging problems.

Firstly, it is necessary to prove that recovering substantial amounts of energy from the ocean shall not affect Earth's current dynamic state. The critical issue here is to prevent disturbance of Earth's rotational speed, which, as we already know, can lead to dramatic climatic transformations.

Secondly, it is necessary to demonstrate that the amount of energy recovered from the environment has a commercial value.

And finally, it is desirable to identify an optimal option of transporting energy to facilities located hundreds and thousands of kilometers away from OTEC plants.

In the following sections of the monograph, we will discuss these problems.

4.1. THE ENERGY CAPACITY OF THE OCEAN AND ATMOSPHERE

Let us estimate approximately the time required for the atmosphere and ocean to increase Earth's rotational speed from 365 to 400 revolutions a year.

We will use available data for this. In particular, the seasonal earthday variations with an amplitude of about 0.5 ms have been estimated to correspond to the rate of change of Earth's rotation kinetic energy equal to [51]

$$N_{0.5} = A/\tau = 10^{15}\ \text{J/s},$$

where A is work, J; τ is time, s.

The notation $N_{0.5}$ means that, to reduce the earthday length by 0.5 ms, an energy source with the capacity of 10^{15} J/s is required [53].

Since 1 J/s = 1 W, we can write

$$N_{0.5} = 10^{3}\ \text{TW}.$$

Let us take the amount of water vaporized annually to be [22]:

$$M = 350{,}000\ \text{km}^3$$

or, in a convenient dimensionality,

$$M = 1.11 \times 10^{10}\ \text{kg/s}.$$

We define the energy capacity of the ocean and atmosphere by the formula

$$N = \eta \times Q,$$

where N is energy capacity, W;

η is the efficiency of converting heat energy to mechanical energy;

Q is the heat flux to the atmosphere with water vapor, W.

In the equatorial zone, water evaporates at 28 °C. For these temperature conditions, using reference data, and neglecting atmospheric pressure, we find the heat of vaporization

$$r = 2{,}425.6 \text{ J/kg}.$$

We calculate the heat flux to the atmosphere with water vapor

$$Q = r \cdot M = 26.91 \text{ TW}.$$

We assume that in action there is only the rotational effect with the efficiency of converting heat energy to mechanical energy in the ocean-atmosphere boundary layer of

$$\eta = 0.25 \text{ \%}.$$

Then we find that the energy capacity, due to water evaporation, is

$$N = \eta \cdot Q = 0.067 \text{ TW}.$$

This value of N obtained is considerably less than $N_{0.5}$.

Here it is necessary to note that the energy capacity depends on the rate of performing work. For a steadily operating system, which the Earth is, the energy capacity is measured by work performed per unit time. Naturally, a system without a high energy capacity can perform the same work $A = 10^{15}$ J over a longer time interval.

Actually, the time has to be increased by a factor of Z, where Z is found from

$$Z = \frac{N_{0.5}}{N} = 1.49 \cdot 10^4.$$

Hence, the ocean and the atmosphere are capable of changing the earthday duration by 0.5 ms during the time

$$\tau' = Z \times \tau = 1.49 \times 10^4 \text{ s},$$

i.e. in about 4.14 hours.

Even after these straightforward calculations, we find that Earth's rotational speed will change by 1 s a year; one revolution in 86,400 years, and by 35 revolutions a year in 3 million years.

However, the Earth at present is in a certain dynamic equilibrium state characterized by a constant rotational speed. The planet spends the greater part of mechanical energy received on moving water and air masses from the poles to the equator and back. The Earth spends a certain amount of the energy generated apparently on preventing synchronization of its rotation with the motion of the closest planets, primarily, with the most massive of them, namely, Jupiter.

One should bear in mind that the bulk of heat energy, which, under certain conditions, is capable of being rapidly converted to kinetic energy of currents, is found in the atmosphere. Under the existing conditions, it is crucial to prevent emergence and growth of glaciers when recovering energy from the ocean. Upon attaining a certain critical mass of ice sheets, the temperature differences in the atmosphere between zones located over seas and mountains shall increase sharply. Growth of glaciers' surfaces shall increase the level of interaction of air currents with the terrestrial surface. Both factors will enhance the impact of compression effects, and the Earth shall start accelerating.

This imposes a ban on siting OTEC plants in areas with maximum activity of compression effects, i.e. in the midlatitudes of the Pacific Ocean and in the northern part of the Indian Ocean.

Based on the same possible climatic change concerns, it is extremely risky to attempt to utilize the energy of the Gulf Stream, the Kuroshio current, the Brazilian and other warm currents for generating electric power.

Hence, at our disposal we have a narrow belt limited by the latitudes 5°N and 5°S. This belt is often called the "hot belt of the planet". Here, the most active natural processes occur, which ensure removal of insolation.

But, in certain periods of the year, the established flow circulation mechanism clearly fails to cope with this problem. As a result, "excess" energy is "ejected" to the midlatitudes in the form of energy of uncontrolled hurricanes and typhoons.

Our task is to tap efficiently this "excess" energy, which, apparently, will not disturb Earth's rotational speed.

Thus, having identified the OTEC plant sites, we have approached, in part, to resolving the first of the problems posed.

The final solution involves a statistical analysis of the amount of kinetic energy removed annually by hurricanes and typhoons from the planet's equatorial belt. The volume of mechanical energy recovered by OTEC plants should not exceed the value found by statistical analysis.

Unfortunately, natural dynamic structures have variable parameters, making it impossible to obtain reliable statistical data. Most likely, the number and capacity of OTEC plants will have to be defined experimentally.

At this phase of investigation, using our general notions about energy processes, we shall attempt to find the minimal amount of energy that can be recovered from the ocean's "hot" belt.

At first sight, it seems that the total energy capacity of the ocean N = 0.067 TW, estimated by the mass of annually vaporized water, is negligible, if compared with the installed capacity of all globally operating electric power plants, equal to N_C = 3 TW [54].

In our case, however, we are dealing with heat energy already accumulated by the ocean over many years of absorbing solar radiation. Warm water can be considered as low-calorific fuel. Let us justify our idea by straightforward calculations.

The solar energy flux density [22] is know to be

$$q = 153.4 \text{ J/m}^2 \cdot \text{s}.$$

The water surface loses as much heat as the ocean receives by solar radiation. About half of the losses are accounted for by reverse radiation, and the remaining part is radiated to the atmosphere through water evaporation, heat transfer and convection.

Let the evaporation losses be

$$q' = 76.7 \text{ J/m}^2 \cdot \text{s}.$$

Let us remind that the water temperature in the surface layer reaches 28 °C, and at the depth of 500 m, it drops to 4 °C. Hence, the effective temperature difference is 24 °C.

In an energy installation operating to the limit thermodynamic cycle, warm water, due to flashing in vacuum, cools to 4 °C.

From reference data we find that each cubic meter of water, when cooled from 28 °C to 4 °C, loses heat in the amount of

$$q'' = 10^8 \text{ J/m}^3.$$

A floating power plant leaves in its wake a water surface layer with the temperature of 4 °C. This results in cessation of apparent surface layer heat losses, with a decrease in evaporation. Water starts absorbing solar radiation in the amount of q'.

Hence, the time required for restoring the initial energy capacity of the selected ocean layer is

$$\tau_L = \frac{q''}{q'} \cdot L,$$

where L is the layer height, m.

For instance, a cubic meter of water shall restore its temperature in

$$\tau'_L = 1.3 \times 10^6 \text{ c}$$

or in 15 days. A layer with the thickness of L = 100 m shall recover its previous state in

$$\tau''_L = 4.1 \text{ years.}$$

Whence it follows that the total capacity of floating OTEC plants should be selected so that the heat concentrated presently in the ocean's equatorial zone be sufficient for generating electric power for 4.1 years. During this period, the Sun will restore the energy capacity of initial energy recovery sites, and the plant flotilla will be able to return to its initial site and sail along its previous course.

Let us determine the installed capacity of OTEC plants.

The water surface of the planet's belt delimited by us above is

$$F = 18 \text{ mln km}^2.$$

This value is approximately equal to 10 % of the ocean's evaporation surface.

The amount of water contained in a surface layer with the thickness of L = 100 m is

$$V = L \times F = 1.8 \times 10^{15} \text{ m}^3.$$

The layer possesses heat energy in the amount of

$$Q'' = q'' \times V = 1.8 \times 10^{23} \text{ J.}$$

Let us assume the value of the minimum efficiency of heat-to-mechanical energy conversion to be at the level of efficiency of the natural thermal compressor acting in mountains

$$\eta = 0.5 \text{ \%.}$$

Then the installed capacity of OTEC plants is

$$N = \frac{\eta \cdot Q''}{\tau''_L} = 6.96 \text{ TW.}$$

This value significantly exceeds the energy capacity of the rotational effect.

Here it is appropriate to cite Ericsson, one of the pioneers of solar radiation engineering: "Archimedes undertook to move the world with a lever. But I maintain that, by concentrating solar heat, one can generate a force capable of stopping the Earth in its track" [55].

Earlier we presumed that the low solar energy flux density on Earth's surface gives no chance for feasible implementation of large-capacity power projects. Thus, to obtain 100 MW from an insolated surface, the accumulating de-

vice area should be 1 km^2. In this case, the energy generated will not recover the capital input. Besides, solar radiation varies not only daily, but is also dependent on the season and the weather conditions [56].

But this reasoning holds only for direct conversion of solar energy to electric or mechanical energy. When utilizing the temperature difference between the ocean water layers, we are dealing with solar energy that has already been accumulated in water in the form of heat. The Sun continuously restores the energy potential of the surface layer.

The power plant has no accumulating device as such, its functions being performed by the ocean's upper water layer. And finally, the water heated in the upper layer does not cool overnight, and inflow of solar radiation to the ocean's equatorial zone shows a weak dependence on the time of the year.

Earth's rotational speed was earlier noted to be extremely sensitive to heat balance changes in the atmosphere and ocean. Therefore, it is desirable to minimize the zone of action of OTEC plants. Further, we will ascertain the Earth's equatorial belt area than can be counted on.

Besides, having proved the commercial value of energy recovered from the ocean's surface layer, we have not yet substantiated the type of engine that would be capable of utilizing low-potential heat efficiently. These issues will be covered in the following section.

4.2. ANALYZING THE LIMIT CYCLES OF OTEC PLANTS

The power plants built earlier, which use the temperature difference between the ocean's upper and bottom water layers, have several critical drawbacks. Thus, for example, utilizing a cycle with steam generation by warm water flashing in vacuum (the Claude plant; the Virginia plant; and the designed, but not built, Abidjan plant) is the least effective method because of the small amount of efficiently utilized heat. Besides, the high metal capacity, the large sizes of wet steam turbines and their small unit capacity involve significant capital input. This imposes additional constraints on the practical solution of this problem [57 to 59].

Power plants with low-boiling working media (ammonia, Freon, butane, propane, carbon dioxide, etc.) make it possible to increase electric power unit generation, and reduce the size and cost of turbines.

These installations, however, have several drawbacks, the major ones being the presence of large-size heat exchange apparatus (heaters and condensers), and irreversible heat losses therein, which are especially significant at small temperature differences between the warm and cold water. This is at-

tested by performance data of plants whose working media are ammonia and Freon. Thus, the OTEC plant erected near the Hawaiian Islands managed to deliver 12 to 15 kW to the electric grid, but spent 35 kW on in-plant demand. The OTEC plant on the Nauru Island has demonstrated a somewhat better performance. Here, under maximum load conditions, electric power generation was 120 kW, and the net power delivered to the grid was 31.5 kW. Commissioning of more powerful plants has been slated. The specialists developing the projects have focused on reducing in-plant electric power demand to 10 % of the energy generated [60 to 66].

However, these plans failed. This can be accounted for by ungrounded transfer of engineering solutions used in conventional power engineering to the area of OTEC plant design. Specifically, the designers of OTEC plants fail to account for the energy constraints associated with utilizing evaporators and steam turbines. The negative features of these constraints become especially evident when utilizing small temperature differences.

In our opinion, the OTEC plant in Fig. 21 is free of deficiencies inherent to power plants with steam turbines [67 to 70].

Warm water from the ocean's upper layers is continuously fed via pipe 6 and hollow shaft 2 to hydraulic steam turbine 5 (in this case, the turbine is designed as a Segner wheel). In the turbine nozzles, the water flow boils and the generated steam expands to the ultimate backpressure. Steam, in expanding, accelerates the steam mixture. The reaction forces arising in Laval Nozzles rotate shaft 2 to drive pump 7 and electric generator 8, wherein mechanical energy is converted to electric energy.

Cold water flows via pipe 4 through hydraulic turbine 3 to chamber 1, its upper part being a condenser. After the steam has condensed, the condensate, together with the cold and warm water flows, is discharged from chamber 1 by pump 7. Chamber 1 is vacuumed by pump 9, which evacuates the non-condensing gases (primarily, carbon dioxide with water vapor released from water) via pipe 10. Further, the gases are delivered via pipe 11 to reactor 12. In the reactor, carbon dioxide reacts with associated water vapor to synthesize hydrocarbons. Here, in reactor 12, the hydrocarbons are polymerized and delivered via pipes 13 and 14 to the warm and cold water flows. The polymers dissolve to reduce water turbulence, which makes it possible to reduce the water flow resistance of the pipelines, turbine paths and the pump.

To set up the plant for operation, it is crucial that the warm water be evacuated previously from the cold-water pipeline. Therefore, a rather powerful external energy source should be available for system start-up. In so doing, electric generator 8 is used as an electric motor.

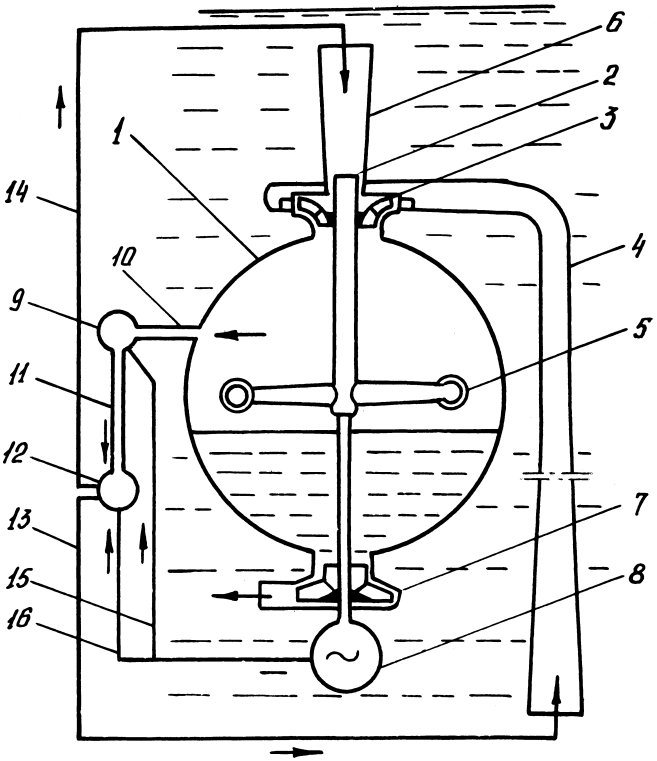

1 — evaporator chamber; 2 — vertical hollow shaft; 3 — hydraulic turbine; 4 — cold water pipe; 5 — hydraulic steam turbine; 6 — warm water pipe; 7 — centrifugal pump; 8 — electric generator; 9 — air pump; 10 and 11 — discharged gases pipe; 12 — reactor; 13 and 14 — liquid polymer pipe; 15 and 16 — electric cable.

Fig. 21. Scheme of an OTEC plant with a hydraulic steam turbine

Cold water is known to have a density higher than warm water does. Under stationary conditions, the cold water level in pipe 4 is about 1 m below the ocean's surface.

Since vacuum is maintained continuously in chamber 1, warm and cold water flows therein by gravity.

In so doing, it was taken into account that mounting the centrifugal pump on one shaft with the heat and hydraulic turbines has the effect that, with plant submersion, centrifugal pump 7 power consumption increases little because the increasing potential energy of the warm and cold water is utilized com-

pletely by turbines 3 and 5 for generating mechanical energy delivered to the pump and the electric generator. Plant submersion to a certain depth makes it possible to evade trouble involving the impact of hurricanes, typhoons and tsunamis on its structure.

The vertical position of the cold water pipe is maintained by making its lower part heavier.

The reaction of the water jet discharged from chamber 1 by pump 7, allows the plant to sail along the right course, ensuring thereby energy "collection" in a specific area of the ocean.

The plant suggested can be manufactured readily; it has a small metal capacity, and its key feature is that it allows efficient utilization of a significantly greater temperature difference as compared to that of steam turbines.

Fig. 22 shows the cycle implemented by the plant suggested.

For comparison, the Claude plant with a steam turbine was selected (Fig. 23); its cycle is shown in Fig. 24.

Both plants are assumed to operate in equal conditions. Warm water is supplied to the plants at the temperature of 28 °C, and cold water is supplied at the temperature of 4 °C.

Water steam, generated by warm water boiling in the hydraulic steam turbine, is then condensed at the temperature of 7 °C by coming into contact with cold water. Hence, the efficient temperature difference utilized by the hydraulic steam turbine is 21 °C.

The process in the prior art plant differs in that water steam is generated a priori in a special evaporator, and only then it is delivered to the steam turbine.

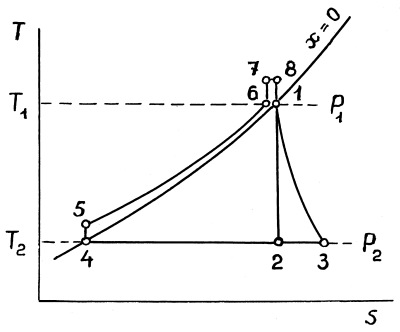

12 – process in the converging part of the Laval nozzle for the ideal cycle, i.e. without friction energy losses (13 – isoenthalpic process of flow throttling); 24 – steam condensation; 45 – pressure boosting with the centrifugal discharge pump (accompanied by a slight temperature rise); 56 – liquid heating with solar radiation; 67 – pressure buildup in turbine's horizontal channels due to centrifugal force; 81 – process in the diverging part of the Laval nozzle.

Fig. 22. Cycle of a power plant with a hydraulic steam turbine in the T–S coordinate system

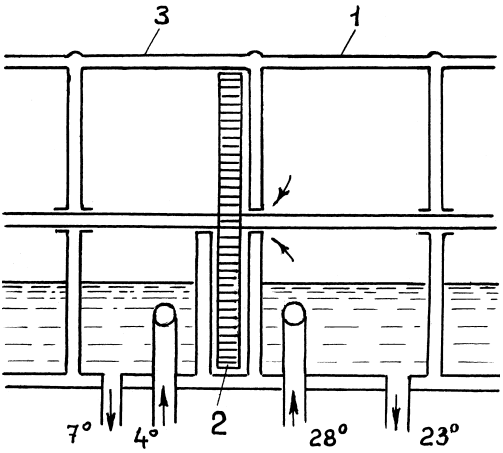

1 — evaporator; 2 — turbine; 3 — condenser.

Fig. 23. Power plant with a steam turbine

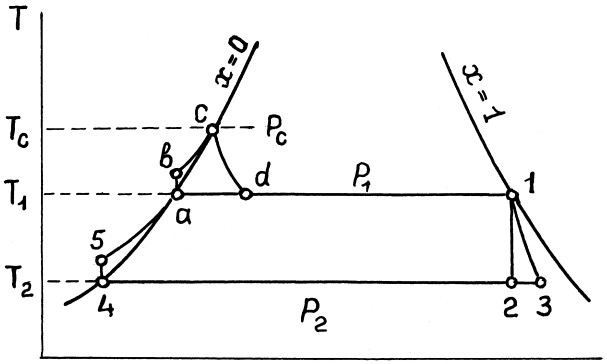

12 — steam expansion process in the ideal cycle (13 — isoenthalpic process of flow throttling); 24 — steam condensation; 45 — pressure boosting (at a slight temperature rise) with the pump evacuating water from the condenser; 5a — water discharged from the condenser is heated by solar radiation; aв — pressure boosting (at a slight temperature rise) with the pump evacuating water from the evaporator; вc — water discharged from the evaporator is heated by solar radiation; cd — isoenthalpic process of water boiling in the evaporator.

Fig. 24. Cycle of a power plant with a steam turbine in the T—S coordinate system

Warm water boiling in the evaporator makes its temperature drop from 28 °C to 23 °C. The steam is condensed downstream the turbine. The condensation temperature is also at the level of 7 °C.

Let us make a preliminary estimate of the efficiency of the suggested and prior art power plants.

4.2.1. First-approximation calculation of the efficiency of electric power generation

The efficiency of power plants is known to be found from dependency [26]

$$\eta = \eta_{н.} \cdot \eta_{t.b.} \cdot \eta_{b.},$$

where $\eta_{н.}$ is the ideal cycle efficiency;

$$\eta_{н.} = \eta_{t} \cdot \eta_{i.e};$$

$\eta_{t.b}$ is the efficiency accounting for different kinds of losses in the turbine building;

η_{b} is the efficiency of the boiler unit, or evaporator.

Evidently, the above expression makes it possible to account for losses at any stage of the plant's working cycle by simply multiplying the right-hand part of the equality by the thermal efficiency, the internal thermal efficiency, the mechanical efficiency, etc.

The thermal efficiency of an ideal triangular cycle (Fig. 22) is equal to

$$\eta'_{t} = \frac{T_1 - T_2}{T_1 + T_2} = 0.036.$$

The internal thermal efficiency of a hydraulic steam turbine is assumed [71] to be

$$\eta'_{i.e} = 0.65.$$

In ideal conditions, the losses in the power plant's machine area shall be within 5%. Hence:

$$\eta'_{t.b} = 0.95.$$

Since in the plant suggested there is no evaporator that generates water steam, this implies that

$$\eta'_{b} = 1.$$

By multiplying the partial efficiency values obtained, we find the total efficiency of a plant with a hydraulic steam turbine

$$\eta' = 2.22\ \%.$$

The same procedure is used to calculate the efficiency of the Claude plant (Fig. 24)

$$\eta''_t = \frac{T_1 - T_2}{T_1} = 0.054.$$

The internal efficiency of a single-stage steam turbine with the capacity of N ≈ 100 MW is equal to [31]

$$\eta''_{i.e} = 0.865$$

The efficiency $\eta''_{t.b}$ remains at the same level as in the previous case.

We estimate the evaporator available heat factor during surface water boiling in process cd (Fig. 24) by the dependency

$$\eta''_b = \frac{c'_c \cdot t_c - c'_a \cdot t_a}{c'_c \cdot t_c - c'_4 \cdot t_4}.$$

Since the water heat capacity, at small temperature differences, changes slightly, we can calculate the evaporator efficiency with a negligible error by the formula

$$\eta''_b = \frac{t_c - t_a}{t_c - t_4} = 0.238.$$

Knowing the values of partial efficiencies, straightforward calculations yield the value of the total efficiency of the prior art plant

$$\eta'' = 1.06\ \%.$$

The ratio of the total efficiency values of the power plants compared is

$$z = \frac{\eta'}{\eta''} = 2.1.$$

Hence, the efficiency of our plant exceeds that of the Claude plant by more than twice. This is not surprising since the bulk of heat inflow with surface water delivered to the evaporator in the prior art installation is returned not utilized to the ocean.

Further, by increasing the accuracy of calculations, and introducing therein energy losses associated with operation of auxiliary equipment, we will attempt to confirm the preliminary conclusions.

4.2.2. Second-approximation calculations of the efficiency of the electric power generation process

We will first consider a power plant with a hydraulic steam turbine.

Following the known procedure, and using data on the thermophysical properties of water and water steam [72], we find the cycle thermal efficiency η'.

For this, we find the entropy of the steam-liquid mixture after adiabatic expansion in process 12 (Fig. 22)

$$S_2 = S'_1 = 0.4088 \text{ kJ/(kg} \times \text{K)}.$$

The entropy of dry steam at pressure $P_2 = 1.0012 \cdot 10^3$ Pa and $t_4 = 7$ °C is equal to

$$S''_2 = 8.9751 \text{ kJ/(kg} \times \text{K)}.$$

The mixture steam content after adiabatic expansion is

$$x_2 = \frac{S_2 - S'_2}{S''_2 - S'_2} = 0.0341.$$

The enthalpy of the steam-liquid flow is

$$i_2 = i'_2 + r_2 \times x_2 = 114.079 \text{ kJ/kg}.$$

The heat drop utilized by the turbine is

$$h' = i'_1 - i_2 = 3.2 \text{ kJ/kg}.$$

The available heat-and-energy difference is

$$\Delta i = i'_1 - i'_4 = 87.866 \text{ kJ/kg}.$$

The thermal efficiency of a cycle with a hydraulic steam turbine is

$$\eta'_t = \frac{h'}{\Delta i'} = 0.0364.$$

Analyzing limit cycles implies introducing into calculations, by definition, the maximum possible relative turbine efficiencies.

For most efficient utilization of the energy of the steam-liquid mixture, the circumferential speed of the reaction turbine should be equal to the relative velocity of the outgoing stream. Under optimal conditions, the overall efficiency of a reaction turbine is $\eta'_{r.e} = 0.828$ [25]. Hence, the maximum amount of mechanical energy generated by the turbine per unit mass of warm water is

$$\eta'_{r.e} \times h' = 2.661 \text{ kJ/kg}.$$

Let us examine energy losses in separate components of the plant.

The water flow resistance of the plant's channels is known to absorb the bulk of available energy. These losses can be reduced by introducing soluble polymers into the flows. Polyethylene oxide, polyacrylamide, guar gum, and other polymers can reduce the fluid resistance factor by three to four times.

Using this method, when utilizing small temperature differences, is impractical because polymers have to be supplied continuously from the land to the OTEC plant.

Meanwhile, this impediment can be easily overcome by utilizing part of the generated electric power for producing soluble polymers in-situ [67 and 73].

Let us recall that each cubic meter of deep-sea water at 4 °C contains 1.5 m^3 of dissolved carbon dioxide [44]. When spent steam is condensed, deep water is heated from 4 °C to 7 °C, resulting in liberation of 0.16 m^3 of carbon dioxide from its each cubic meter. This gas, together with part of the water vapor, is evacuated continuously from the condenser by the vacuum pump.

An empirical equation established for a droplet deaerator was used for a tentative estimate of the water degassing efficiency. Having defined the volume of liberated gases, we calculated the amount of energy consumed by the vacuum pump [74 and 75].

Installing on the plant platform a reactor for producing hydrocarbons from carbon dioxide and water vapor, followed by their polymerizing and introducing into the warm and cold water flows, allows to reduce the resistance of the motors, the discharge pump and pipelines to these flows.

Dissolved carbon dioxide synthesis proceeds to the equation [76]

$$2CO_2 + 2H_2O + 1{,}2\ \text{kJ} \rightarrow C_2H_4O + 5^{1/2}O_2.$$

The reaction yields ethylene oxide, and after polymerizing, it yields polyethylene oxide.

The amount of heat required for producing polymer additives was calculated by the above formula. Producing 1 kg of polyethylene oxide was found to require 20,000 kJ of heat. The effect of reducing the resistance of the channel water flow is achieved by adding thereto polyethylene oxide for 0.0025 %.

As mentioned earlier, mounting a fluid and heat engine on one shaft with the centrifugal pump allows for efficient utilization of both heat and potential energy of water flows to the vacuum system. Adding polymers to the flows, and optimizing the plant components' layout, minimizes water transport energy losses.

Table 2 summarizes the estimated values of energy consumed by separate kinds of equipment.

The total energy consumption of the plant auxiliary equipment is $Q' = 0.911$ kJ/kg or 34.26 % of the generated power.

Whence the plant economic efficiency is

$$\eta'_{EE} = \frac{\eta'_{r.e} \cdot h' - Q'}{i'_1 - i'_4} = 1.99\ \%.$$

Table 2

Energy consumption of plants' auxiliary equipment

Parameter description	Hydraulic steam turbine		Steam turbine	
	kJ/kg	%	kJ/kg	%
Total amount of available energy	2.661	100	1.096	100
Warm water discharge	0.125	4.72	0.123	11.2
Cold water discharge	0.087	3.28	0.203	18.5
Discharging gases	0.196	7.4	0.051	4.63
Producing polymers	0.502	18.86	–	–

The efficiency of a plant with a steam turbine is estimated along similar lines.

The enthalpy of a steam-liquid mixture, when water boils in the isoenthalpic process cd (Fig. 24), is found from the equality

$$i_d = i'_c = 117.31 \text{ kJ/kg}.$$

The heat of vaporization at pressure $P_1 = 2.863 \cdot 10^3$ Pa and $t_1 = 23$ °C is

$$r_d = 2{,}446.8 \text{ kJ/kg}.$$

The amount of steam generated in the evaporator xd is found from expression

$$i_d = i'_d + r_d \times x_d.$$

$$x_d = 0.00854.$$

The amount of warm water required for generating 1 kg of dry steam is

$$M = \frac{1}{x_d} = 117.09 \text{ kg}.$$

Being vaporized, steam is separated from water, so the calculation has to be done for 1 kg of dry steam.

The enthalpy and entropy of dry steam at the temperature of $t_1 = 23$ °C are $i''_1 = 2{,}543.2$ kJ/kg; and $S''_1 = 8.6014$ kJ/(kg • K), respectively.

After adiabatic expansion, the wet steam entropy is

$$S_2 = S''_1.$$

Value x_2 is found from equation

$$x_2 = \frac{S_2 - S'_2}{S''_2 - S'_2} = 0.9578,$$

where S''_2 and S'_2 are steam and water entropy, respectively, at the temperature of t = 7 °C.

After expansion, the wet steam enthalpy is

$$i_2'' = i_2' + r_2 x_2 = 2{,}290.12 \text{ kJ/kg}.$$

The energy that can be generated theoretically by 1 kg of steam is

$$h_S = i_1'' - i_2'' = 137.9 \text{ kJ/kg}.$$

The energy generated theoretically by 1 kg of warm water is

$$h_W = \frac{h_S}{M} = 1.177 \text{ kJ/kg}.$$

The thermal efficiency of a cycle with an evaporator and steam turbine is

$$\eta_t'' = \frac{h_W}{i_c' - i_4'} = 0.0134.$$

For the most effective utilization of the steam jet energy, the circumferential velocity of a blade should theoretically be one-half of the absolute velocity of the discharge jet. Under these conditions, the effective relative efficiency of an active turbine, whose guide vanes angles are 15°, is equal [25] to

$$\eta_{r.e} = 0.932.$$

Hence, the maximum amount of energy generated by 1 kg of warm water is

$$\eta_{r.e} \times h_W = 1.096 \text{ kJ}.$$

Further, we calculate the energy consumption of auxiliary equipment, and enter it to Table 2. The plant's total consumption for in-plant demand is Q" = 0.376 kJ/kg or 34.35 %.

Whence the economic efficiency of the Claude plant is

$$\eta_{EE}'' = \frac{\eta_{r.e} \cdot h_b - Q''}{i_c' - i_2'} = 0.82 \text{ \%}.$$

The ratio of the efficiencies of the power plants compared is

$$Z = \frac{\eta_{EE}'}{\eta_{EE}''} = 2.42.$$

Hence, the economic efficiency of the power plant suggested exceeds that of the prior art one by a factor of 2.4.

The thin surface layer, possessing heat energy, cannot generate the unit capacity of a power plant. A 100 MW power plant is a rather large facility. Its overall dimensions are as follows: the warm water pipe diameter is 7.0 m; and the hydraulic steam turbine diameter is 17 m. The steam-liquid mixture is discharged from six nozzles. The outlet section diameter of each nozzle is 4.5 m.

Development of the most powerful energy source on Earth, as evident, depends entirely on developing a boiling liquid-driven thermal engine.

Due to this, it makes sense to review studies focused to improving hydraulic steam turbines of different types.

4.3. IMPROVING HYDRAULIC STEAM TURBINES

In elementary thermodynamic models, the steam-liquid flow is assumed to possess the qualities of a homogeneous medium. To evaluate actual non-equilibrium flows, it is necessary to identify the properties of a homogeneous quasi-equilibrium flow. The system of equations of a one-dimensional flow has a general character in no way constrained by the absolute value of steam dryness.

Meanwhile, there is a qualitative difference between expansion of a homogeneous flow away from the lower and upper boundary curves. At isoenthalpic expansion of a two-phase flow, liquid evaporates away from curve $x = 1$, whereas similar flow expansion of the flow away from curve $x = 0$ involves steam moistening. As a result, in the former case the degree of steam dryness increases, and in the latter one, it decreases.

However, the basic flow regularities undergo greater change in actual non-equilibrium flows. Therefore, when analyzing two-phase media, a comparatively well investigated area of low moisture-content steam is distinguished from the high moisture-content steam area. Let us expand our ideas on the latter, still comparatively little investigated area of flow motion.

Investigating the features of boiling flow discharge in a transparent Laval nozzle model proved the presence of a metastable core. The clearly defined flow separation into a steam-liquid wall layer and a superheated liquid slug flow in its central part precludes efficient utilization of the available heat energy [27].

When testing an experimental stand, we registered a decrease in the internal thermal efficiency $\eta_{i.e}$ of a hydraulic steam turbine with growth of the efficient temperature difference. This phenomenon was noted earlier to be associated with two causes: firstly, with an increase in two-phase flow velocity, the liquid fails to boil completely in the diverging part of the Laval nozzle, and secondly, the losses in the reaction turbine are caused by impact of the steam-liquid jet exiting one nozzle on the casing of the other.

By selecting the geometric dimensions of Laval nozzles, we managed to achieve an internal efficiency equal to $\eta_{i.e} = 38$ to 42 %. An attempt to reduce the impact of metastability by decreasing the diameter of Laval nozzles failed to yield positive results. In this case, the flow resistance of a hydraulic steam turbine increases as much as to stop circulation.

The capacity of the hydraulic steam turbine we tested was N = 3 kW. The same level of the internal efficiency value, but at higher temperature differences, was achieved when operating an impulse hydraulic steam turbine with a capacity of up to N = 70 kW.

The nozzle diaphragm of the impulse turbine comprises a set of nozzles whose channels are shaped as two truncated pyramids connected with a rectangular constant-area section. The nozzle diaphragm is also equipped with steam generating grids [77 and 78].

The intended refinement of the hydraulic steam turbine design will make it possible to increase its internal efficiency by about 20 % [71].

These measures should be followed up by process-focused methods of increasing the internal efficiency. For instance, employing soluble polymers at OTEC plants will lead both to turbulence mitigation and to reduction in water metastability. The point is that long polymer molecules represent a foreign body in water, so their surface promotes the process of steam bubble formation.

Employing acoustic radiators with a frequency of several hundred kilohertz ensures complete decay of the core stream of superheated liquid. The latter makes it possible to implement in one accelerating nozzle assembly a combination of the triangular water boiling process and the circular process of two-phase flow compression, also having a triangular shape [79 and 80].

The elementary scheme of a combined nozzle is shown in Fig. 25. Fig. 26 shows its ideal thermodynamic cycle in the T–S coordinate system.

The heated liquid (the active agent) flows at temperature T_1 to nozzle 1 of the Laval type, where it boils to the isoentropic process cd. The cooling liquid (the passive agent) at temperature T_e flows into chamber 2 and accelerates in its converging part. In chamber 3, the flows mix and the bulk of the steam phase condenses. Steam condensing ceases in cylindrical channel 4. The outlet section Z of channel 4 is arranged so that jet 5 impinges on blades 6 of turbine 7 at the required angle. In this case, Pelton turbines are used as the movers [81].

At steady operation of the combined nozzle, in section K, downstream mixing chamber 3, a droplet-steam mixture at temperature T_3 is developed. For the process in the guide case to be thermodynamically reversible, the active agent in the mixing chamber should be cooled along line de, corresponding to the passive agent heating process. Area efabcde corresponds to the available energy that can be utilized for increasing the ultimate head of the mixture created (here we neglect the energy consumed by feed pumps for effecting processes ab and ef).

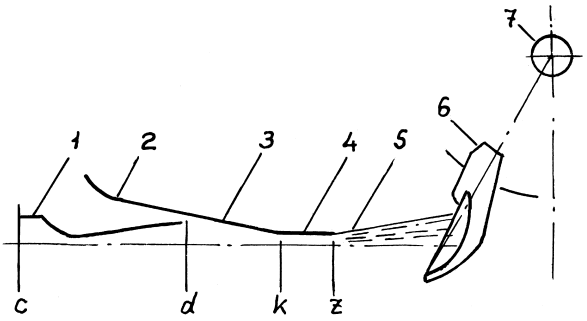

Fig. 25. Scheme of a combined nozzle

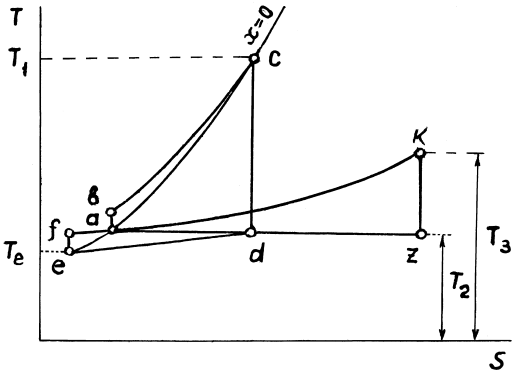

Fig. 26. Thermodynamic cycle of a combined nozzle in the T–S coordinate system

To implement the process described, in the mixing chamber, between sections d and к, the pressure should increase from level P_2, corresponding to saturation at temperature T_2, to the level corresponding to temperature T_3. Then the active agent should have to expand in nozzle 1 to the minimal pressure in the mixing chamber, corresponding to temperature T_2.

In actual conditions, the pressure in the mixing chamber remains practically steady. The active agent expands by isoentrope cd from pressure P_1 to pressure P_3, corresponding to saturation temperature T_3. The process of active agent cooling in the mixing chamber will correspond to isobar (isotherm) da.

The available work will decrease by value fadef. The amount of heat transferred to the passive agent will increase respectively. At steady temperature T_3, the passive agent mass increases. In the generalized diagram, line fk corresponds to heating of the increased amount of cooling liquid. In this case, entropy growth characterizes irreversibility linked to actual temperature drops between the agents being mixed.

Refining speed-up nozzle design should be focused to bringing the value of area abcda, representing the kinetic energy of the boiling steam-liquid flow in section d, closer to that of area efkze, equivalent to the kinetic energy of the high-velocity droplet-liquid flow in section Z.

Analysis of experimental data on testing separate components of the combined nozzle has demonstrated good agreement with the theory of its design [27].

For us, the generalized process considered is also interesting because it allows developing a similar procedure of natural heat compressor analysis, where moist air currents, in flowing into mountain ridges, convert their kinetic energy into potential energy.

Let us remind that, in the acceleration nozzle, the main kinds of losses are metastability ones. To increase the effectiveness of nozzle 1, it can be fitted with a steam-generating grid, acting, at the same time, as an acoustic radiator.

Employing the nozzle developed will increase the turbine internal efficiency apparently to $0.7 < \eta_{i.e} < 0.75$.

With this in view, the expected economic efficiency of an OTEC plant should be within $1.5 < \eta_{EE} < 1.7$ %.

The working medium volume at the end of expansion is a key characteristic of a turbine. The vacuum water steam involves an increase in the overall size of a hydraulic steam turbine by about three times as compared to an equal-capacity steam turbine employed currently at TPPs. However, if we compare metal capacity per unit energy generated, then it is also necessary to take into account the metal capacity of auxiliary equipment. An OTEC plant has a degasser, a pump for water discharge, a vacuum pump, and pipelines. A TPP's auxiliary equipment comprises mechanisms for coal preparation, crushers, driers, boiler units, heat recovery units, condensers, gas treatment and ash disposal systems, and pipelines. Hence, the unit metal capacity of a TPP exceeds that of an OTEC plant by dozens of times. Besides, coal mining and transportation also add up to the metal capacity.

Mines, railways, electric power plants and their waste piles occupy huge land areas, which could be used for agricultural purposes. Fuel combustion at power plants involves emission of toxic, carcinogenic and mutagenic substances to the atmosphere. OTEC plants are free of these drawbacks.

At first sight, it appears that a plant with an efficiency of less than 2 % is non-profitable. The energy cycle currently accepted by industry, which ultimately uses solar energy, is known to have a still lower efficiency. The first chain of this cycle — photosynthesizing plants — are known to assimilate only 1 to 3 % of incident solar light. The energy they accumulate is concentrated in coal deposits and, possibly, in oil and gas. The next chain is heat engines that utilize these kinds of fuel with an efficiency of about 30 %. As a result, the cycle overall efficiency is $\eta = 0.02 \cdot 0.3 = 0.006$, i.e. less than 1 %.

Besides, the key factor, when comparing the efficiency of a TPP and an OTEC plant, is the cost of feed stock fuel. With account of this factor, the scales clearly tip in favor of the OTEC plant advantages.

What remains is to adjust the results of the estimated ocean area to be utilized. The values η_{EE} found allow reducing the OTEC plant operational area by a factor of three.

Here we emphasize that thermohaline circulation can restore the surface layer cooled by an OTEC plant most likely in a matter of months. Hence, it is unlikely that OTEC plants will have to be sailed over large ocean expanses.

4.4. PRODUCTION OF ENERGY-INTENSIVE SUBSTANCES AT OTEC PLANTS

So, OTEC plants can generate a practically unlimited amount of comparatively cheap energy.

Straight away, one is tempted to deliver this energy to land in the form of conventional energy carriers and utilize them in industrial processes currently employed. However, at this point we are faced with a question: "To what extent are we right in prolonging the life of an outdated fleet of automobiles, and of thermal power plants with their excessively high energy consumption?"

For example, by producing hydrocarbons at OTEC plants and delivering them to land, we thereby will make for keeping in operation TPPs and transportation vehicles, which recover fuel energy with an efficiency of only 15 to 30 %. In this case, toxic, carcinogenic and mutagenic substances will continue to accumulate in the environment, not to mention an increase in concentration of greenhouse gases.

In converting, say, to hydrogen, TPPs and automobiles will be capable of generating electric power in fuel cells with an efficiency of 65 to 70 % without polluting the atmosphere with their emission.

But, in solving the problem of generating cheap electric power in this manner, we are bringing ourselves to another extreme, viz. to creating favor-

able conditions for preserving the steel, chemical and food production facilities in their current state.

About 15 to 25 % of machines and equipment are known to be removed annually from the World's metal stock, amounting to billions of tons, due to corrosion and damage caused by poor strength properties of the materials used. Huge funds are spent on restoring the operational capabilities of the metal stock. This can be overcome by launching production of non-corrosive, high-strength and special alloys directly at the OTEC plant site. These materials could then be delivered to land for manufacturing machinery, computers, metal structures, etc.

It also makes no sense to supply agricultural production with cheap hydrogen. Here this high-calorific and ecologically clean fuel will be used with negligible effect for plowing land, sowing, fertilizing and harvesting.

Economically, it would be more profitable to produce proteins and other hydrogen-based products directly at the OTEC plants, bypassing the stages of generating, transporting and consuming energy carriers.

A similar conclusion can be drawn, if we analyze production of different kinds of chemical products, such as fertilizers, rubber, plastics, synthetic fibers, paint, etc.

Whence it follows that it would be practical to locate the most energy-intensive and ecologically hazardous industrial facilities as well as some agricultural production facilities directly on floating OTEC plant platforms.

However, let us revert to the problem whose solution can be promising for making qualitative changes in the technologies of base industry and transport branches. The case in point is production and utilization of cheap hydrogen.

In the following is a list of production areas where hydrogen is used currently.

The chemical, petroleum refining, coal and petrochemical industries:

– synthesis of ammonia, hydrogen chloride, and methanol; hydrocarbon recovery (reforming), including by-products required for producing rubber, nylon, aniline, polyurethane, dyes and soap;

– producing small volumes of special chemical agents, in particular, hydrogen peroxide for manufacturing Persol and washing powders;

– in hydrocracking processes and processes of hydrofining refined oil products and lubricants, and recovery of catalysts;

– producing liquid fuel from coal [82 and 88].

The microbiology industry:

– protein production based on hydrogen-oxidizing bacteria [89].

The food industry:

– hydrating vegetables, animal fat and lard for solidification. Margarine is the main product. Hydrogen consumption depends on the value of iodine in oils to be hydrated; cod-liver oil (e.g. anchovy oil) has iodine content higher than vegetable fat (oil), hence, it requires more hydrogen.

Metallurgy and machine building:

– employing hydrogen as a reduction medium in steel production and in metalworking, especially in the process of bright annealing of stainless steel, and in fritting;

– in production of high-purity silicon for making microcontacts in the electronic industry;

– in incandescent lamp, electronic tube and picture tube production processes;

– for hydrogen and hydrogen-oxygen cutting and welding of metals, and for deposition of corrosion-resistant coatings;

– in production of floated glass [88, 90 and 92].

Power engineering and transport:

– extraction and processing of uranium; obtaining superheated steam when combusting hydrogen in oxygen; cooling rotor and stator windings in electric generators;

– using hydrogen as basic fuel in transport vehicle engines, and as an initiating additive to hydrocarbon fuels [88, 93 and 97].

Astronautics, aviation, water and air transport, and the meteorological service:

– fuel for rocket and aviation engines; a reagent in chemical current sources; gas for filling airships, radiosondes and spherical piloting shells; and gas for marine lifting devices [88, 95, 98 and 103].

As evident, the unique properties of hydrogen make it an indispensable agent in the majority of chemical and metallurgical processes; allow using it as a high-calorific and ecologically pure fuel; and make it a premium gas for water and air transport vehicles.

Of course, reducing the cost of hydrogen will extend the areas of its application as well as increase its consumption volume.

Let us discuss the options of utilizing OTEC plant energy with account of the required hydrogen production volumes. Electric energy generated by OTEC plants was suggested earlier to be used for producing chemical products and fuel (hydrogen); for oxidizing and deoxidizing organic substances, extracting gold, iodine and other substances from seawater, and especially for binding nitrogen [104]. Accumulated solar energy was also suggested to be used for air liquefaction. Liquid air can then be vaporized by ambient heat and

used in air engines [105]. Feasibility studies were carried out for two kinds of production processes, viz. gaseous (or liquid) hydrogen and nitrogen production [106]. Their common features are as follows: electric power generation, water desalination and hydrogen production. In so doing, the cost of power devices, electric generators, desalinating installations and electrolyzers was taken from manufacturer's data sheets.

In case of liquid hydrogen production, the cost of its liquefying plant was taken into account; and for ammonia production, the cost of the equipment for air separation and reactors, where air nitrogen reacts with hydrogen, was accounted for.

The study was based on two plants with the capacity of 100 and 500 MW each, located at the distances within 185.2 km to 1,852 km from the shore.

We calculated the cost of transporting hydrogen and liquid ammonia by pipelines submerged to about 456 meters and by ocean barges, as a second option. In the latter case, the cost of building wharfs was taken into account.

The cost of energy transported from the OTEC plant turned out to be slightly higher than that of synthetic fuels produced from coal. Thus, the cost of methanol produced from coal was 6.0 to 7.5 dollars per MW • h, whereas the cost of liquid hydrogen was 10 to 15 dollars per MW • h. As to the cost of ammonia transported to the shore, it was within 270 to 277 dollars per ton. For comparison, the cost of ammonia produced with hydrogen recovered from methane was 190 to 200 dollars per ton in 1975. The estimates took account of the cost of energy generated by steam turbines. But if we take into account that hydraulic steam turbines generate 1.5 to 2 times cheaper electric energy, the cost of products produced on land and in the ocean turn out to be equal.

Focusing to transporting hydrogen to land is not altogether justified. The major drawback of hydrogen in this case is its low density. A cubic meter of gaseous hydrogen weighs only 0.089 kg. Presently, hydrogen is transported in cylinders at the pressure of 150 atm. The weight of each cylinder is 85 kg, the weight of hydrogen therein being only 0.5 kg. At such weight ratios, it is inefficient to transport gaseous hydrogen in tankers.

Liquid hydrogen at 20 K has the density of 71.3 kg/m^3, also requiring large-capacity tankers for transportation. Besides, floating plants have to be equipped with special hydrogen liquefaction installations, and tankers have to be equipped with thermostatic controllers for maintaning the hydrogen temperature at 20 K. Handling liquid hydrogen is also known to be extremely fire-hazardous.

The challenges presented can be met if electric power generated by OTEC plants were used for reducing oxides of some substances. After this, these sub-

stances could be transported by common tankers to the mainland where, in special reactors, they would react with water to yield hydrogen and oxides. Hydrogen could further be used as a fuel for different power installations. To this end, one can use, for example, lithium, boron, magnesium, aluminum, calcium, silicon and other elements [93]. The practical effectiveness of the method suggested for transporting energy to the mainland can be proved by example of the aluminum and water reaction equation

$$2Al + 3H_2O = Al_2O_3 + 3H_2 + Q_p.$$

The weight amounts of reacting substances are such that, for obtaining 1 kg of hydrogen, 9 kg of aluminum are needed, the reaction yielding heat in the amount of $Q_p = 15{,}155$ kJ per each kilogram of aluminum. This heat can also be recovered effectively.

Taking into account that 1 kg of liquid hydrogen occupies the volume of $14 \cdot 10^{-3}$ m^3, and 9 kg of aluminum occupy $3.1 \cdot 10^{-3}$ m^3, a tanker transporting aluminum can deliver to the shore ten times more energy than when transporting liquid hydrogen. When hydrogen is substituted for coal, oil and gas, several hundred million tons of aluminum will be required for transporting energy from an OTEC plant to land. The challenge of producing such an amount of aluminum consists in that the reserves of high-quality bauxites are rather limited on Earth. Therefore, further we will discuss a more feasible option of obtaining energy-accumulating substances from low-calorific coal.

The reserves of this, so-called low-calorific, or high ash-content coal, are hundreds of billions of tons. Carbon content in this coal is about 30 to 60 %, the remaining part being accounted for by inorganic substances, mainly, aluminum, silicon and iron oxides.

The power economy is known to utilize coal with a minimum content of inorganic compounds (less than 10 %).

Coke, made of coal for metallurgy, even more so does not admit for any oxide inclusions.

Hence, the huge reserves of low-calorific coal turn out to be unclaimed.

However, the optimal combination of carbon and oxides gives low-calorific coal the most valuable properties of stock for producing necessary alloys and alloying components.

Producing one ton of ferro-silicon-aluminum (FSA) alloy requires, on the average, three tons of high ash-content coal and 12 MW of electric power.

When carbon interacts in ore heat furnaces with aluminum, silicon and iron oxides, a significant amount of gaseous carbon oxide is released, making it possible to produce 0.6 tons of methanol per each ton of alloy manufactured.

The impurities contained in coal pass in part to the alloy, this affecting its activity.

A high reactivity, when reacting with water and liberating hydrogen, was demonstrated by an alloy with the following ratio of components, mass percentage: iron 5.0 to 15.0; aluminum 3.0 to 20.0; calcium 0.1 to 1.0; sodium 0.01 to 1.00; copper 0.1 to 3.0; and silicon the rest; as well as by the alloy [108]: iron 5.0 to 15.0; aluminum 3.0 to 20.0; calcium 0.1 to 1.5; boron 0.01 to 3.2; potassium 0.01 to 1.0; and silicon the rest.

Prior to being used in hydrogen reactors, the alloys are previously hardened at 1,600 to 1,750 °C, or high-speed hardening is used to obtain an amorphous structure [109 to 111].

The coal waste of domestic concentration plants has been analyzed recently to determine the possibility of its usage as stock for FSA alloy fusion [112].

Concurrent with refining the alloy composition and extending the stock range for alloy production, several transport and stationary hydrogen reactors were developed and tested [113 to 116].

Besides being used in the power engineering, transport and coal industries, launching wide-scale production of the FSA alloy on OTEC plants will encompass metallurgy as well. The point is that this alloy is already being used in significant volumes for deoxidizing, modifying and alloying steel [117 and 118]. In the future, FSA will replace expensive coke.

At present, we are developing an aluminum-making technology by centrifuging the FSA alloy. This work will make it possible to supply machine building with cheap structural aluminum as well as with corrosive-resistant fused silica-aluminum alloys.

Earlier we concluded that there is no pressing need for large-scale production of currently known energy carriers at OTEC plants. However, hydrocarbon synthesis in the ocean is appropriate when the case in point is producing food. For this, it would suffice to install a plant for continuous cultivation of hydrogen bacteria on the plant platform. Hydrogen-oxidizing bacteria are known [119 and 120] to be capable of synthesizing a biomass rich in protein, vitamins, as well as other products from a primitive gaseous medium by utilizing the hydrogen oxidation energy. The gas mixture feeding the bacteria contains 50 to 60 % H_2, 20 to 30 % O_2, and 2 to 5 % CO_2. The first two elements can be obtained by water electrolysis, and carbon dioxide can be obtained by degassing depth water. The bacteria are cultivated in a nutrient mineral medium containing nitrogen, phosphorous, sulphur, potassium, magnesium and other substances. The majority of these can be found in seawater, or obtained from air.

The average specific caloric content of the hydrogen bacteria biomass is 22,175 kJ/kg, the hydrogen oxidation energy recovery factor achieving the level of 24.5 %. Under optimal cultivation conditions, hydrogen bacteria excrete in significant amounts only the hydrogen oxidation product — water.

One-tenth of a kilogram of hydrogen bacteria protein contains the full daily diary intake of essential amino acids required for Man. Biosynthesis of 1 kg of dry biomass requires 40 to 50 kW • h of electric power. A 100 MW OTEC plant can produce 2,000 tons of dry biomass per hour.

Hence, not so far is the time when fleets of tankers carrying low-calorific coal will sail to OTEC plants, and return fully loaded with valuable metallurgical and chemical products, which can also be used as energy carriers.

Part of the tankers will bring in proteins and other sea products.

The low cost of electric power generated by OTEC plants will drive industry and agriculture to the expanses of the ocean.

CONCLUSIONS

Thermodynamic analysis has shown that, under specific conditions, the ocean and the atmosphere are capable of changing Earth's axial rotational speed by 30 to 40 revolutions a year in three million years.

To prevent Earth's rotational speed variation, OTEC plants should be sited in a narrow belt of the equatorial zone.

Approximately three times more energy can be generated from the ocean's equatorial belt area of 5 mln km^2 than the entire world's power generating plants do currently.

The most promising engine capable of effectively utilizing the small temperature differences between ocean water layers is a boiling-water turbine.

It would be practical to locate energy-intensive production of alloys, proteins and chemical products on OTEC plantships. The stock for alloy fusion could be low-calorific coal supplied to OTEC plantships by tankers.

The alloys produced at OTEC plants are of multiple purposes. They can be used as steel deoxidizers, stock for making aluminum, as well as an active reagent for producing hydrogen from water.

Mass production of cheap hydrogen can have a quantitative impact on the technologies of producing industrial and agricultural products, as well as improve the performance of transport vehicles.

AFTERWORD TO PART I OF THE BOOK

In this section, it is common practice to summarize the problems presented in the book. But since brief conclusions have been drawn up in each chapter, there is no sense in repeating them.

It seems more practical to discuss here the measures to be taken to resolve the problems of developing renewable energy sources.

From the material presented herein, it is clear how many-sided the posed problem is. As to its economic value, however, harnessing the unlimited reserves of natural energy is no less important than, for instance, exploring space or the ocean deep.

The impact of the technique suggested on Earth's climate will become evident immediately as soon as the first fleet of OTEC plantships sets to sea.

From the laws of thermodynamics it follows that climatic cycles on Earth are irreversible, and as soon as warming or cooling sets in, it is impossible to stop them. This fact has to be taken for granted, and siting of new cities and industrial facilities should be carried out with account of changes expected in Nature.

Let us see how much of a hazard the warming taking shape on Earth is.

The World Ocean is known to occupy more than 71 % of Earth's surface. If we subtract from the remaining part areas covered with glaciers, deserts, mountains, swamps and tundra with its permafrost, where life is practically impossible, it will turn out that humankind huddles on 10 % of Earth's surface. This is the cause of serious conflicts over pieces of land, which also, as a rule, are unfit for normal life.

In Earth's history, however, there were periods when the temperature of the World Ocean's surface layers was about the same on the equator and in the polar regions. In this tropical period, the biosphere extended its domain from the North to the South Pole.

The thawing of glaciers in the Antarctica and Greenland has been estimated to increase the level of the World Ocean by 60 m, which will flood part of Earth's lowlands. Indeed, this will actually occur. But concurrent improvement of circulation of waters in the World Ocean will make available for humankind the boundless expanses of the Antarctica and Greenland, and will make Siberia, Alaska and Canada's North fit for life. Finally, having at our disposal powerful natural energy sources will make it possible to cover the Sahara with a network of canals with circulating water flows, and to change it to a blossoming garden. Floating cities will also resolve part of the territorial problems.

New opportunities will open in utilizing the biological resources of the vast polar regions.

Maybe the UN should change their focus from settling long-standing territorial conflicts to resolving problems of effective utilization of mainland.

Therefore, it is necessary to involve interested countries in developing OTEC plants.

Earlier the research team leaded by the author suspended the development of concrete pilot OTEC plants. The reason was one, namely, the cost of security measures required to protect the floating OTEC plant from external attack turned out to be commensurable with the cost of the plant itself. However, in the light of numerous human casualties and material expenditures on eliminating the consequences of recent disasters connected with the explosion of the nuclear power plant reactor and destruction of skyscrapers, the OTEC plant security expenditures are not believed to be so excessively high now.

Building OTEC plants will eliminate conflicts involving energy sources.

Apparently, there is an impending necessity to coordinate more closely the efforts of power engineers with research activities of meteorologists and oceanologists. We cannot afford losing the opportunity of regulating Earth's climate by floating OTEC plants.

The author invites readers to participate in a discussion on the problems highlighted in the book. Part II of the monograph will be published in about six months, allowing to include in its Appendix the most interesting comments on Part I. It should be mentioned that the first phase of discussions was held after information on the method of recovering natural energy [68, 69 and 121 to 125] had been published. The most astonishing fact was that specialists participating in the discussion failed to make a distinction between the thermal efficiency of a turbine ht and its internal efficiency η_{ie} [126 and 127]. It is understood that similar comments, contradicting in essence the laws of physics, will not be included in the Appendix to Part II of the book.

Here it is appropriate to remind the expected participants of the discussion once more of the fact that the material presented in the monograph is merely a theory reflecting the most probable mechanism of terrestrial processes observed. Only integrated in-depth studies in the active zones of the atmosphere and ocean, combined with measuring Earth's rotational speed, would be able to either confirm or refute the theory suggested.

In this connection, the author expresses his hope that specialists interested in participating in the discussion will suggest their experimentally proven models of natural phenomena.

Following up on Part II of this monograph, the author intends to publish the book Accumulated Energy in two parts: — Part I. Thermodynamics of the Biosphere. Part II. Electrochemical and High-Temperature Power Plants.

The Appendix of this book will contain readers' comments on Part II of the monograph Renewable Energy.

At the same time, the author reserves the right to respond to the most active critics of his theory.

Incidentally, the technique of applying the methods of thermodynamics for analysis of industrial and natural processes is currently at an extremely low level.

Thus, in spite of the long period that has elapsed since the author published the thermodynamic theory of natural circulation of flows [95], in the majority of higher education institutions, including NTU "KhPI", the students continue to study the erroneous hydrodynamic method of design of flow circuits in steam generators and evaporators.

In all the literature on meteorology and oceanology reviewed, the author also failed to find thermodynamical analytical calculations of significant value. Among Ukrainian scientists, oceanologist V. Shuleikin managed to approach closest to comprehending the thermodynamic basics of natural processes. However, absence of a baseline theoretical model of dependence of natural events on Earth's rotational speed, and of an experimental verification of this thesis kept V. Shuleikin from completing his studies successfully.

Hence, a finding suggests itself that a course on thermodynamical methods of analyzing natural and industrial processes should be introduced to the curriculum of higher education institutions. It may be that increasing the level of knowledge in a so abstract and hard-to-understand subject as thermodynamics will help scientists and engineers focus public opinion to addressing the challenge we are facing. In this case, obviously, it will be easier to persuade potential investors to commit funds for developing full-scale OTEC plant projects. It is these circumstances that made the author compile this textbook for the academic course.

REFERENCES

1. J. W. Gibbs. Works in Thermodynamics. — M.; L.: State Publishers of Technical and Theoretical Literature (Gosizdat Tekhniko-Teoret. Lit.), 1950. — 492 pp. (Translated to Russian).

2. Landau L. D. Collected works in 2 vols. / Ye.M. Lifschitz (Editor). — M.: Nauka Publishers, 1969. — Vol. 1 — 512 pp.

3. Problems in Modern Cosmology / V.A. Ambartsumian (Editor). — M.: Nauka Publishers, 1972. — 472 pp.

4. Hawking S. A. Brief History of Time: From the Big Bang to Black Holes. — M.: Mir Publishers, 1990. — 168 pp. (Translated to Russian).

5. Porolo L.V. Air-Gas Liquid Lifts (Air-Gas Lifts). Basics of Theory and Design Methods. — M.: Mashinostroenie Publishers, 1969. — 160 pp.

6. Inv. Cert. 324,028 (U.S.S.R.). Method for Solution Stripping / B.A. Troshenkin, A.V. Gerasimenko and P.G. Luchin. — Publ. in Bull. Inv., 1972. № 2.

7. Yastrezhembsky A.S. Engineering Thermodynamics. — M.; L.: Gosenergoizdat Publishers, 1960. — 495 pp.

8. Styrikovich M.A., Martynova O.I. and Miropol'sky Z.L. Steam Generation Process at Electric Power Plants. — M.: Energia Publishers, 1969. — 312 pp.

9. Idel'chik I.E. Reference Book for Hydraulic Resistances. — M.: Mashinostroenie Publishers, 1975. — 559 pp.

10. Wallis G. One-Dimensional Two-Phase Flow. — M.: Mir Publishers, 1972. — 440 pp. (Translated to Russian).

11. Investigation in Turbulent Flows of Two-Phase Media / Kutateladze (Editor). — Novosibirsk, Inst. for Heat Physics SO AN U.S.S.R., 1973. — 315 pp.

12. Bakulin P.I., Kononovich E.V. and Moroz V.I. Course in General Astronomy. — M.: Nauka Publishers, 1974. — 512 pp.

13. Zharkov V.N. Internal Structure of Earth and Planets. — M.: Nauka Publishers, 1983. — 416 pp.

14. Gal'perin I.I., Il'insky A. A., Almazov O. A., et al. Liquid Hydrogen. — M.: Khimia Publishers, 1980. — 228 pp.

15. Properties of Condensed Hydrogen and Oxygen Phases. — Kyiv, Naukova Dumka Publishers, 1984. — 240 pp.

16. Thermodynamic Properties of Separate Substances. — M.: Nauka Publishers, 1978. — Vol. 1, Book 1. — 496 pp.; vol. 1, Book 2. — 328 pp.

17. Properties of Liquid and Solid Hydrogen. — M.: Standards Publishers, 1969. — 136 pp.

18. Bronstein V.A. Hypotheses on Stars and the Universe. — M.: Nauka Publishers, 1974. — 384 pp.

19. Shuleikin V.V. Physics of the Sea. — M.: Publ. AN U.S.S.R.., 1953. — 990 pp.

20. Lacombe H. Cours D'Oceanographie Physique. — M.: Mir Publishers, 1974. — 496 pp. (Translated to Russian).

21. Interaction of the Ocean and Environment / A.I. Duvanin (Editor). — M.: Publ. Moscow University, 1982. — 214 pp.

22. Lacombe H. Les Energies de la Mer. — L.: Gidrometeoizdat Publishers, 1972. — 128 pp. (Translated to Russian).

23. Khundjua G.G., Andreev Ye.G. and Skorokhvatov N.A. On-Site Observations of the Radiation Temperature and Effective Radiation of the Sea's Surface // Thes. Rep. 7th Plenum of Task Group for Ocean Optics of AS U.S.S.R. Commission for World Ocean Problems. Optical Methods of Investigating Oceans and Inland Basins, Oct. 1980. — Tallinn, 1980. — pp. 205–208.

24. Formation, Structure and Fluctuation of Ocean's Upper Thermocline. — L.: Gidrometeoizdat Publishers, 1971. — 144 pp.

25. Schulle W. Technische Thermodynamik. — M.; L.: Gosenergoizdat Publishers, 1934. v.1. — Book 2. — 262 pp. (Translated to Russian).

26. Zysin V.A. Combined Steam-Gas Plants and Cycles. — M.; L.: Gosenergoizdat Publishers, 1962. — 186 pp.

27. Boiling Adiabatic Flows / V.A. Zysin (Editor). — M.: Atomizdat Publishers, 1976. — 152 pp.

28. Inv. Cert. 401,369 (U.S.S.R.) Stripping apparatus / P.G. Luchin and B.A. Troshenkin. — Publ. in Bull. Inv., 1973, № 41.

29. Dryndrozhek E.I. Critical Velocity of a Two-Phase Flow. — In book: Heat Transfer, Hydrodynamics and Thermophysical Properties of Substances. — M.: Nauka Publishers, 1968. — pp. 87–100.

30. Zysin V.A. and Barilovich V.A. Experimental Investigation of Hydraulic Steam Turbine. — M.: Energomashinostroenie Publishers, 1973. — 1. — pp. 4–6.

31. Losev S.M. Steam Turbines. — M.; L.: Gosenergoizdat Publishers, 1954. — 368 pp.

32. Eisenstein M.D. Centrifugal Pumps for the Petroleum Industry. — M.: Gostoptekhizdat Publishers, 1957. — 364 pp.

33. Baranovsky N.V., Kovalenko L.M. and Yastrebenetsky A.R. Plate-Type and Helical Heat Exchangers. — M.: Mashinostroenie Publishers, 1973. — 160 pp.

34. Hydrodynamics of Interphases: Coll. articles 1979–1981. Transl. from English / Compiled by Yu.A. Buevich and L.M. Rabinovich. — M.: Mir Publishers, 1984. — 210 pp.

35. Jaluria Y. Natural Convection: Heat and Mass Transfer. — M.: Mir Publishers, 1983. — 400 pp. (Translated to Russian).

36. Lorenz E.N. The Nature and Theory of the General Circulation of the Atmosphere. — L.: Gidrometeoizdat Publishers, 1970. — 260 pp. (Translated to Russian).

37. Vitvitsky G.N. Atmosphere Circulation in the Tropics. — L.: Gidrometeoizdat Publishers, 1971. — 144 pp.

38. Perry A.H. and Walker J.M. The Ocean–Atmosphere System. — L.: Gidrometeoizdat Publishers, 1979. — 196 pp. (Translated to Russian).

39. Lebedev I.V., Treskunov S.L. and Yakovenko V.S. Elements of Fluidic Automatics. — M.: Mashinostroenie Publishers, 1973. — 360 pp.

40. Sokolov Ye. Ya., Zinger N.M. Fluidic Devices. — M.: Energoatomizdat Publishers, 1989. — 352 pp.

41. Inv. Cert. 760,537 (U.S.S.R.). Hydrogen-Generating Installation / A.N. Podgorny, I.L. Varshavsky, B.A. Troshenkin, et al. — Publ. in Bull. Inv., 1981, № 33.

42. Steam Locomotives. / S.P. Syromiatnikov and A.A. Chirkov (Editors). — M.: Transzheldorizdat Publishers, 1949. — 692 pp.

43. Troshenkin B.A. and Gal'tsov V.Ya. Concentrating Latex in Rising Upflow. — Khim. i Neft. Mashinostroenie Publishers, 1966. — 8. — pp. 26–27.

44. Smirnov G.N. Oceanology. — M.: Vyssh. Shkola Publishers, 1974. — 344 pp.

45. Barbara McKee. Solutions for the 21st Century. Zero Emissions Technologies for Fossil Fuels. Technology Status Report. — U.S.A. International Energy Agency, 2002. — 48 p.

46. Tarling D. and Tarling M. Continental Drift. A Study of the Earth's Moving Surface. — M.: Mir Publishers, 1973. — 104 pp. (Translated to Russian).

47. Yasamanov N.A. Prehistoric Earth's Climates. — L.: Gidrometeoizdat Publishers, 1985. — 296 pp.

48. Nazarov G.N. Glaciation and Geological Development of Earth. — M.: Nedra Publishers, 1971. — 152 pp.

49. The Winters of the World. / Edited by B. John. — M.: Nedra Publishers, 1982. — 336 pp. (Translated to Russian).

50. Munk W. and Macdonald G. The Rotation of the Earth. — M.: Mir Publishers, 1964. — 384 pp (Translated to Russian).

51. Kiselev V.M. Irregularity of Earth's Diurnal Rotation. — Novosibirsk: Nauka Publishers SO, 1980. — 160 pp.

52. Tugarinov A.I. General Geochemistry. — M.: Atomizdat Publishers, 1973. — 288 pp.

53. Sena L.A. Physical Units and Their Dimensionalities. — M.: Nauka Publishers, 1988. — 432 pp.

54. More Than Enough? An Optimistic Assessment of World Energy. / Edited by R. Clarke. — M.: Energoatomizdat Publishers, 1984. — 216 pp. (Translated to Russian).

55. Gurevich B.Z. Energy of Invisible Light. — M.: Nauka Publishers, 1973. — 144 pp.

56. Kapitsa P.L. Experiment, Theory and Practice. — M.: Nauka Publishers, 1981. — 496 pp.

57. History of Engineering. Chief Editorial Board for General Technical Literature and Monographs. ONTI NKTP U.S.S.R.. M. — L., 1935. Issue 3. — 249 pp.

58. W. D. Mets. Ocean Temperature Gradients: Solar Power From the Sea./ Solience. — 1973, vol. 180, p. 1266–1267.

59. Riffaud C. Demain le Mer. — L.: Gidrometeoizdat Publishers, 1978. — 272 pp. (Translated to Russian).

60. L. L. Booda. An Ocean-Based Solar-to-Hydrogen Energy Conversion Concept. — Sea Technol., 1974, 15, 2, P. 21–24.

61. Mitsui T., Ito F., Seya Y. and Nakamoto Y. Outline of the 100 km OTEC Pilot Plant in the Republic of Nauru. IEEE Transactions on Power Apparatus and Systems, 1983, Vol. Pas — 102. — № 9. P. 3167–3171.

62. Weymueller Carl R. Oceans of Energy — Power From Warm Water./ Weld. Des and Fabr., 1982. — 55. — № 4. P. 92–94.

63. Floating Power Stations./ Engineering, 1982. — 222. — № 5. — 357 p.

64. Vershinsky N.V. Energy of the Ocean. — M.: Nauka Publishers, 1986. — 152 pp.

65. Lenmard D. E. OTEC Developments Out of Europe // EET Rerour: Technol. Assess. Conf., Honolulu, Haw., Jan. 22–26, 1989: Proc. — Honolulu (Haw.), 1989. — P. 6/2–6/12.

66. Dokukin I.P. Thermodynamic Analysis and Optimization of Electric Power Plants Utilizing Sea Water Temperature Differences for Generating Electric Power/ Teploenergetika, 1992. — 10. — p. 68–75.

67. Inv. Cert. 730,992 (U.S.S.R.) Method for Utilizing Ocean Water Temperature Differences/ A.N. Podgorny, I.L. Varshavsky and B.A. Troshenkin. — Publ. in Bull. Inv., 1980. № 16.

68. Troshenkin B.O. Utilizing Ocean Heat for Hydrogen Production/ Visnyk Akademii Nauk Ukr. S.S.R., 1979. — 10 — p. 22–30.

69. Troshenkin B.A. Utilizing Low-Potential Heat for Recovering Hydrogen from Water. — Kharkov, 1980. — 38 pp. (Preprint AN Ukr. S.S.R., Inst. for Mechanical Engineering Problems; № 106)

70. Troshenkin B. A. Energy Utilization of Ocean Heat // The First International Conference on New Energy Systems and Conversions: Poster Session Wind, Ocean, Biomass and Other Renewable Energies: Yokohama National University. June 27 (Sun) – 30 (Wed), Japan, 1993, 4127.

71. Barilovich V.A., Smirnov Yu.A. and Starikov V.I. On the Heat Efficiency of Geothermal Electric Power Plants / Teploenergetika, 1985. — № 11. — p. 54–56.

72. Rivkin S.L. and Aleksandrov A. A. Thermophysical Properties of Water and Water Vapor. — M.: Energia Publishers, 1980. — 424 pp.

73. Experimental Investigation in Wall Turbulent Flows. // S.S. Kutateladze, B.P. Mironov, V.Ye. Nakoriakov and Ye.M. Khabakhpashaeva. — Novosibirsk: Nauka Publishers SO, 1975. — 168 pp.

74. Oliker N.N. and Permiakov V.A. Thermal Deaeration of Water at Thermal Power Plants. — L.: Energia Publishers, 1971. — 186 pp.

75. Strakhovich K.I., Frenkel' M.I., Kondriakov I.K, et al. Compressor Machines. — M.: Gostorgizdat Publishers, 1961. — 600 pp.

76. Vol'fkovich S.I, Rogozin Z.A. Rutsenko Yu.M., et al. General Chemical Technology. — M.: Goskhimizdat Publishers, 1955. — vol. 2. — 848 pp.

77. Starikov V.I. Analyzing the Structure of a High-Moisture Steam-Drop Flow in Curved Channels for Developing Methods of Designing Hydraulic Steam Turbines Intended for Operation at GeoTES: Author's Abstract Thesis Cand. Sc. (Eng.). — L.: Leningrad Polytechnic Institute, 1986. — 16 pp.

78. Inv. Cert. 121,6376 (U.S.S.R.) Two-Phase Turbine / V.A. Barilovich, V.I. Starikov, V.K. Smekhov, et al. — Publ. in Bull. Inv., 1986, № 9.

79. Pazhi D.G. and Galustov V.S. Fundamentals of Liquid Spraying Techniques. — M.: Khimia Publishers, 1984. — 256 pp.

80. Inv. Cert. 397,667 (U.S.S.R.) Method of Turbine№ Driven Set Operation / V.A. Zysin, V.A. Barilovich, Sh.B. Batuev, et al. — Publ. in Bull. Inv., 1973, № 37.

81. Edel' Yu.U. Pelton Turbines. Theory, Analysis and Design. — M.-L.: Mashgiz Publishers, 1963. — 250 pp.

82. Lebedev V.V. Physico-Chemical Fundamentals of Processes of Recovering Hydrogen from Water. — M.: Nauka Publishers, 1969. — 136 pp.

83. Cherny I.R. and Cherny Yu.I. Current State of and Trends in Developing Hydrogen Production. — M.: TsNIITEneftekhim, 1976. — 80 pp.

84. Pis'men M.K. Hydrogen Production in the Oil/Petroleum Refining Industry. — M.: Khimia Publishers, 1976. — 208 pp.

85. Chemierohstoffe aus Kohle / Trans. from German to Russian. Edited by I.V. Kalechitsa. — M.: Khimia Publishers, 1980. — 616 pp.

86. Kapustin M.A. et al. Carbon Oxide and Hydrogen-Prospective Stock for Synthesizing Petrochemical Products. — M.: TsNIITEneftekhim, 1981. — 60 pp.

87. Stepanov A.V. Producing Hydrogen and Hydrogen-Containing Gases. — Kiev: Nauk. Dumka Publishers, 1982. — 312 pp.

88. Hydrogen. Properties, Production, Storage, Transportation, and Utilization.: Handbook / D.Yu. Gamburg, V.P. Semyonov, et al. — M.: Khimia Publishers, 1989. — 672 pp.

89. Volova T.G., Terskov I.A. and Sid'ko F.Ya. Microbiological Hydrogen-Based Synthesis. — Novosibirsk: Nauka Publishers SO, 1985. — 118 pp.

90. Rykalin N.N., Legasov V.A., Manokhin A.I., et al. Prospects of Utilizing Nuclear Energy in Metallurgy / Nuclear-Hydrogen Power Engineering and Technology. — M.: Atomizdat Publishers, 1979. — № 2. — p. 16–31.

91. Hasui A. Deposition Techniques (Tekhnika Napylenia). — M.: Mashinostroenie Publishers, 1975. — 288 pp. (Translated from Japanese to Russian).

92. Martin J. Hydrogen — the Next Five Years in the UK // Chem. and Ind., 1984. — № 2. — P. 46–49.

93. Varshavsky I.L. Energy-Accumulating Substances and their Utilization. — Kiev: Nauk. Dumka Publishers, 1980. — 240 pp.

94. Shpil'rein E.E., Malyshenko S.P. and Kuleshov G.G. Introduction to Hydrogen Power Engineering. — M.: Energoatomizdat Publishers, 1984. — 264 pp.

95. Troshenkin B.A. Circulation and Film Evaporators, and Hydrogen Reactors. — Kiev: Nauk. Dumka Publishers, 1985. — 174 pp.

96. Kozin L.F. and Volkov S.V. Hydrogen Power Engineering and Ecology. — Kiev: Nauk. Dumka Publishers, 2002. — 336 pp.

97. Mischenko A.I. Utilizing Hydrogen for Automobile Engines. — Kiev: Nauk. Dumka Publishers, 1984. — 142 pp.

98. Paushkin Ya.M. The Chemistry of Reactive Fuels. — M.: Publ. AS U.S.S.R., 1962. — 436 pp.

99. Bogotsky V.S. and Skundin A.M. Chemical Current Sources. — M.: Energoatomizdat Publishers, 1981. — 360 pp.

100. Field Gas-Recovery Hydrogen Installations. / Description and Operating Instructions. — M.: Voyenizdat Publishers of Peoples' Defense Commissariat, 1943. — 128 pp.

101. Instructions on Safe Operation of Cylinder Gas Generators AVG-45 and Oxygen Cylinders . — M.: Gidrometeoizdat Publishers, 1978. — 32 pp.

102. Kalekin O.Yu., Gerasimenko V.Ye., Poda V.B., et al. Submergible Hydrogen Generators // Abstract. Rep. All-Union Conf. "Khimreaktor-10", 25 Sept. 1989. — Kuibyshev-Togliatti, 1989. — III. — p. 139–145.

103. Figichev L.I. Emergency Recovery and Ship Lifting Gear. — L.: Sudostroeine Publishers, 1979. — 30 pp.

104. E. Brauer. Verfahren zur Ausnutzung der Temperaturunter-schiede von in der Natur vorkommenden Wassermassen, Patentschrift, № 457,085, kl. 46d, gr. 18,1928.

105. Inv. Cert. № 66,738 (U.S.S.R.). Method of Accumulating Recoverable Energy. G.M. Strongin. — Publ. in Bull. Inv., 1964, № 15.

106. A. Konopka, A. Talib and N. Biederman. The 1st World Hydrogen Energy Conference, 1–3 March, 1976, Miami, Florida, Vol. II, 1B-19–1B-39.

107. Inv. Cert. 1,675,199 (U.S.S.R.) Alloy for Producing Hydrogen / M.L. Khazin, N.Yu. Negodiayev, B.A. Troshenkin, et al. — Publ. in Bull. Inv., 1991, № 33.

108. Inv. Cert. 1,754,643 (U.S.S.R.) Alloy for Producing Hydrogen / A.L. Zavialov, M.L. Khazin, B.A. Troshenkin, et al. — Publ. in Bull. Inv., 1992, № 30.

109. Inv. Cert. 1,699,896 (U.S.S.R.) Method for Obtaining Hydrogen / A.L. Zavialov, V.I. Zhuchkov, B.A. Troshenkin, et al. — Publ. in Bull. Inv., 1991, № 47.

110. Inv. Cert. 1,832,113 (U.S.S.R.) Method for Obtaining Hydrogen / A.L. Zavialov, V.I. Zhuchkov, B.A. Troshenkin, et al. — Publ. in Bull. Inv., 1993, № 29.

111. Troshenkin B.A. and Troshenkin V.B. Heat and Mass Transfer During Hydrogen Emission in Reactions of Amorphous-Crystalline Alloys With Water // Inzhenerno-Fizichesky Zhurnal, 1996. — 69. — № 6. — p. 1006–1008.

112. Litvinenko A.I., Gromov V.A., Yanko S.V., Kabanov A.I. and Troshenkin B.A. Requirements to Coal Waste Utilized for Fusion of Ferro-Silica-Aluminum // Metallurgy. Proc. Zaporozhye State Engineering Academy, 2003. — Issue 7. — p. 38–40.

113. Troshenkin B.A. Reactors for Recovering Hydrogen from Water with Energy-Accumulating Substances // Vopr. Atom. Nauki i Tekhniki. Ser. Atom.-Vodorod. Energetika i Tekhnologia. — 1977. — Issue. 2 (3). — p. 171–172.

114. Troshenkin B.A. and Yurchenko A.P. Certain Methods of Affecting Processes Yielding Toxicity of Transportation Vehicles Exhaust Gases // Abstr. Rep. All-Union Conf. "Protecting the Air Basin from Pollution with Toxic Emission of Transport Vehicles, 12–14 Oct. 1977. — Kharkov, 1977. — p. 113–117.

115. Jurmanov V. A. and Troshenkin B. A. Automatic Facility for Generation of Hydrogen from Water by Using Aluminium/Silicic Fusion // World Meteorological Organization. Instrument and Observing Methods Report № 49. Papers presented at the WMO Technical Conference on Instruments and Methods of Observation (TECO-92), Vienna, Austria, 11–15 May, 1992. — WMO/TD — № 462. — P. 77–80.

116. Troshenkin V.B. Upgrading the Process and Reactor for Generating Hydrogen from Water by Using Alloys Obtained from the Inorganic Part of Coal: Author's Abstract Thesis. Cand. Sc. (Eng.). — Kharkov: Kharkov State Polytechnic University, 1999. — 16 pp.

117. Druinsky M.I. and Zhuchkov V.I. Producing Complex Ferroalloys from Kazakhtan's Mineral Stock. — Alma-Ata, Publication Nauka Publishers Kazakh S.S.R., 1988. — 208 pp.

118. Tsymbal V.P., Bogomiakov V.P., Tolymbekov M.Zh., et al. Effectiveness of Utilizing Ferrosilicon Aluminum for Deoxidizing Steel // Stal'. — 2000. — № 6. — p. 24–26.

119. Terskov I.A., Gitel'zon I.I., Sid'ko F.Ya., et al. The Physiological and Biochemical Characteristics of Growth and the Technique of Cultivating Hydrogen-Oxidizing Bacteria in a Perfusion Culture // Izv. AN U.S.S.R., Ser. Biological Nauka Publishers. — 1977. — p. 541–550.

120. Shmelev-Shampanov O.A., Redikul'tsev Yu.V., Semenov Ya.V., et al. Autotrophic Growth of Hydrogenomonas Eutropha at Optimal Gas Supply // AN U.S.S.R., Microbiology. — 1976. — v. XV. — Issue. 3–6. — p. 389–393.

121. Podgorny A.N., Varshavsky I.L. and Troshenkin B.A. Effective Method of Utilizing the Temperature Difference Between Ocean Water Layers. Abstr. Rep. 1st All-Union Conf. "Problems in Scientific Research in World Ocean Studies and Development. Integrated Problems in Protecting and Utilizing Ocean Waters", 28 Sept.–2 Oct.1976. — Vladivostok, 1976 — p. 67–70.

122. Troshenkin B.A. The Technology of Utilizing Ocean Heat. Abstr. Rep. 4th All-Union Conf. "Problems in Scientific Research in World Ocean Studies and Development. Integrated Problems in Energy Engineering Utili-

zation of Sea Water", 25–28 Oct. 1983. — Vladivostok, 1983 — P.1 — p. 119–120.

123. Troshenkin B.A. Utilizing Ocean Heat for Generating Hydrogen. Issues in Nuclear Science and Engineering. — M.:IEA. I.V. Kurchatova, 1977 — 2(3). — p. 164–165.

124. Troshenkin B.A. Cities in the Ocean. — Khimia i Zhyzn' (Chemistry and Life), 1978. — 8. — p. 34–37.

125. Safronov V. Cities-Power Plants in the Ocean. — Nauka i Suspil'stvo (Science and Society), 1987. — 3. — p. 32–35.

126. Likhosherstnykh G.V. In a Quest for Energy. — Tekhnika Molodiezhi (Technology for Youth), 1983. — 11. — p. 26–29.

127. Shpil'rein E.E. and Semenov A.M. Paraenergetics or How Not to Search for Energy. — Energia, 1984. — 4. — p. 38–47.

CONTENTS

In the design of the book the following photographs were used:
Front cover — Hurricane Hugo/Geos-7/Enhanced Satellite Image/
NASA Goddard Space Flight Center/Laboratory for Atmosphere.
Back cover — Mountain Tetnuldi in Svanetia, Georgia.
Photo by E. Derlemenko.

Please address your comments and requests to:

A.N. Podgorny Institute for Mechanical Engineering Problems
of NAS of Ukraine
Dmitria Pozharskogo Str., 2/10
61046, Kharkov
Ukraine

Additional copies of the book can be ordered at the same address.
The books are delivered on prepayment terms.

Наукове видання

Б.О. Трошенькін
Термодинаміка атмосфери та океана. Океанічні електростанції
(англійською мовою)

Відповідальний за випуск *Г.Є. Лискова*

Підписано до друку 25.12.2003 р.
Формат 60x84/16. Папір офсетний. Друк різографічний. Гарнітура Літературна.
Ум.друк.арк. 5,8. Обл.-вид.арк. 5,0. Тираж 1000 прим. Зам. №

ТОВ "Видавництво "Форт".
Свідоцтво про внесення до Державного реєстру видавців
ДК № 333 від 09.02.2001 р.
61023, м. Харків, а/с 10325. Тел. (0572) 14-09-08